AD-A040 205 NAVAL POSTGRADUATE SCHOOL MONTEREY CALIF F/G 20/13
SOME EXPERIMENTAL OBSERVATIONS OF DROPWISE CONDENSATION OF STEA--ETC(U)
MAR 77 J L MORGAN

UNCLASSIFIED NL

1 OF 2
ADA
040205

AD A040205

NAVAL POSTGRADUATE SCHOOL
Monterey, California

DDC
JUN 6 1977
C

THESIS

SOME EXPERIMENTAL OBSERVATIONS OF DROPWISE CONDENSATION OF STEAM

by

James Larry Morgan

March 1977

Thesis Advisor: P. J. Marto

AD No.
DDC FILE COPY

Approved for public release; distribution unlimited.

UNCLASSIFIED

SECURITY CLASSIFICATION OF THIS PAGE (When Data Entered)

REPORT DOCUMENTATION PAGE		READ INSTRUCTIONS BEFORE COMPLETING FORM
1. REPORT NUMBER	2. GOVT ACCESSION NO.	3. RECIPIENT'S CATALOG NUMBER
4. TITLE (and Subtitle) (6) Some Experimental Observations of Dropwise Condensation of Steam.		5. TYPE OF REPORT & PERIOD COVERED (9) Master's Thesis; March 1977
		6. PERFORMING ORG. REPORT NUMBER
7. AUTHOR(s) (10) James Larry Morgan		8. CONTRACT OR GRANT NUMBER(s)
9. PERFORMING ORGANIZATION NAME AND ADDRESS Naval Postgraduate School Monterey, California 93940		10. PROGRAM ELEMENT, PROJECT, TASK AREA & WORK UNIT NUMBERS
11. CONTROLLING OFFICE NAME AND ADDRESS Naval Postgraduate School Monterey, California 93940		12. REPORT DATE (11) March 1977
		13. NUMBER OF PAGES (12) 130 p.
14. MONITORING AGENCY NAME & ADDRESS(if different from Controlling Office)		15. SECURITY CLASS. (of this report) Unclassified
		15a. DECLASSIFICATION/DOWNGRADING SCHEDULE

16. DISTRIBUTION STATEMENT (of this Report)

Approved for public release; distribution unlimited.

17. DISTRIBUTION STATEMENT (of the abstract entered in Block 20, if different from Report)

18. SUPPLEMENTARY NOTES

19. KEY WORDS (Continue on reverse side if necessary and identify by block number)

Dropwise condensation

20. ABSTRACT (Continue on reverse side if necessary and identify by block number)

Using a tiltable steam condenser test section, the parametric effects of heat flux, non-condensable gas, promoter, condenser surface thermal resistance, and surface inclination were studied on a 3.18 mm thick flat copper plate and on 0.051 mm thick foils of copper and titanium.

Any non-condensable gas concentration, however small, reduces the heat transfer coefficient significantly during → next page

DD FORM 1 JAN 73 1473 (Page 1)

EDITION OF 1 NOV 65 IS OBSOLETE

S/N 0102-014-6601

251454 mdy 1

(20. ABSTRACT CONTINUED)

cont →

dropwise condensation. Non-condensable gases also cause large surface temperature fluctuations, resulting in difficulties of accurately measuring heat transfer coefficients. The recorded data for the heat transfer coefficient of this experiment is lower than previous investigations, possibly due to a concentration of non-condensable gases which resulted from the low steam velocity past the condenser surface or due to the effects of the thin condenser surfaces used.

With a vertical, copper surface, the heat transfer coefficient increases by a factor of five when the condenser surface thickness increases from 0.051 mm to 3.18 mm. The heat transfer coefficient is higher for dropwise condensation on copper than for titanium with mixed condensation. Surface inclination from the vertical position decreases the heat transfer coefficient by as much as 50 percent.

Approved for public release; distribution unlimited.

Some Experimental Observations of Dropwise Condensation of Steam

by

James Larry Morgan
Lieutenant, United States Navy
B.S., Mississippi State University, 1969

Submitted in partial fulfillment of the requirements for the degree of

MASTER OF SCIENCE IN MECHANICAL ENGINEERING

from the

NAVAL POSTGRADUATE SCHOOL

March 1977

Author James Larry Morgan

Approved by: P. J. Marto
Thesis Advisor

Allen E. Fuhs
Chairman, Department of Mechanical Engineering

Robert R. Fossum
Dean of Science and Engineering

ABSTRACT

Using a tiltable steam condenser test section, the parametric effects of heat flux, non-condensable gas, promoter, condenser surface thermal resistance, and surface inclination were studied on a 3.18 mm thick flat copper plate and on 0.051 mm thick foils of copper and titanium.

Any non-condensable gas concentration, however small, reduces the heat transfer coefficient significantly during dropwise condensation. Non-condensable gases also cause large surface temperature fluctuations, resulting in difficulties of accurately measuring heat transfer coefficients. The recorded data for the heat transfer coefficient of this experiment is lower than previous investigations, possibly due to a concentration of non-condensable gases which resulted from the low steam velocity past the condenser surface or due to the effects of the thin condenser surfaces used.

With a vertical, copper surface, the heat transfer coefficient increases by a factor of five when the condenser surface thickness increases from 0.051 mm to 3.18 mm. The heat transfer coefficient is higher for dropwise condensation on copper than for titanium with mixed condensation. Surface inclination from the vertical position decreases the heat transfer coefficient by as much as 50 percent.

TABLE OF CONTENTS

I. INTRODUCTION ---------- 15

A. DESCRIPTION OF THE CONDENSATION PROCESS ---- 16

1. Filmwise Condensation ---------- 17

2. Dropwise Condensation ---------- 20

a. The Film Theory ---------- 20

b. The Nucleation Theory ---------- 21

c. Description of Dropwise Condensation ---------- 22

3. Mixed Condensation ---------- 24

B. A REVIEW OF DROPWISE CONDENSATION LITERATURE ---------- 25

C. OBJECTIVES OF THIS WORK ---------- 33

II. DESCRIPTION OF EXPERIMENTAL APPARATUS ---------- 35

A. STEAM SYSTEM COMPONENTS ---------- 35

1. Boiler Section ---------- 35

2. Steam Ejection System ---------- 36

B. CONDENSER TEST SECTION ---------- 37

1. Condensing Chamber ---------- 38

2. Baffle Housings ---------- 39

3. End Caps ---------- 39

4. Observation Port ---------- 40

5. Illumination Port ---------- 40

6. Condensing Chamber Insert and Clamps --- 41

7. Cooling Water Director ---------- 41

8. Pressure Couplings ---------- 42
9. Test Surfaces---------- 43
C. INSTRUMENTATION ---------- 44
1. Temperature Measurement System ---------- 44
a. Thermocouples ---------- 44
b. Quartz Crystal Thermometer ---------- 47
c. Liquid Crystals ---------- 48
2. Flowmeter ---------- 51
3. Mercury Manometer ---------- 51
D. PHOTOGRAPHIC EQUIPMENT ---------- 51
III. EXPERIMENTAL PROCEDURES ---------- 54
A. TEST SURFACE PREPARATION ---------- 54
1. For Filmwise Mode ---------- 54
2. For Dropwise Mode ---------- 55
3. Application of Liquid Crystals ---------- 57
B. HEAT TRANSFER DATA REDUCTION PROCEDURES ----- 58
1. Heat Flux Determination ---------- 58
2. Temperature Determination ---------- 59
3. Steam Velocity Determination ---------- 60
4. Steady State Determination ---------- 61
5. Photographic Procedures ---------- 61
IV. PRESENTATION AND DISCUSSION OF RESULTS ---------- 63
A. GENERAL ---------- 63
B. QUALITATIVE OBSERVATIONS ---------- 63
1. Liquid Crystals ---------- 63
2. High-speed Motion and Still Pictures ---- 65
3. Brush Recorder Temperature Traces ------- 65

C. FILMWISE CONDENSATION RESULTS ---------- 66

D. HEAT TRANSFER DATA PRESENTATION AND DISCUSSION ---------- 66

1. Effects of Thermal Properties of the Condenser Surface ---------- 67

2. Effects of Non-Condensable Gas --------- 69

3. Transient Effects ---------- 71

4. Effect of Condensation Mode ---------- 71

5. Surface Inclination Effects ---------- 74

V. CONCLUSIONS AND RECOMMENDATIONS ---------- 76

A. CONCLUSIONS ---------- 76

B. RECOMMENDATIONS FOR FURTHER WORK ---------- 77

APPENDIX A: THERMOCOUPLE APPLICATION PROCEDURES ----- 79

APPENDIX B: CALIBRATION OF INSTRUMENTS ---------- 81

1. Thermocouples ---------- 81

2. Quartz Crystal Thermometer ---------- 82

3. Flowmeter ---------- 82

APPENDIX C: PROCEDURES FOR USING AND INTERPRETING THE BRUSH RECORDER ---------- 84

APPENDIX D: UNCERTAINTY ANALYSIS ---------- 86

LIST OF REFERENCES ---------- 123

INITIAL DISTRIBUTION LIST ---------- 130

LIST OF TABLES

Table

I. Thermocouple Correction Values ---------- 92

II. Quartz Crystal Thermometer Correction Values - 93

III. Summary of Data Runs ---------- 94

IV. Flowmeter Calibration Summary ---------- 95

V. Data Calculations with Uncertainty Limits ---- 96

LIST OF FIGURES

Figure	Title	
1	Schematic of Experimental Apparatus	97
2	Photographic View of Experimental Apparatus	98
3	Details of Boiler Joint/Steam Petcock Valve	99
4	Details of Condensing Chamber	100
5	Details of Baffle Housing	101
6	Details of End Cap	102
7	Details of Observation Port	103
8	Details of Condensing Chamber Insert	104
9	Details of Cooling Water Flow Director	105
10	Details of Condenser Pressure Couplings	106
11	Close-up Photograph of the Condenser Section	107
12	Thermocouple Arrangement on Test Surfaces	108
13	Photograph of Dropwise Condensation of Steam on a Vertical Copper Plate with a Heat Flux of 460 kW/m^2 and a ΔT of 9.1 °C	109
14	Photograph of Dropwise Condensation of Steam on a Horizontal (Facing Down) Copper Plate with a Heat Flux of 370 kW/m^2 and a ΔT of 19.0 °C	110
15	Temperature Fluctuation on 0.051 mm Plain Copper Foil as Recorded by Thermocouple 6	111
16	Temperature Fluctuation on 0.051 mm Titanium Foil as Recorded by Thermocouple 6 After Prolonged Boiling	112
17	Temperature Fluctuation on 0.051 mm Titanium Foil as Recorded by Thermocouple 6	113
18	Effect of Thermal Resistance on Heat Transfer Coefficient During Dropwise Condensation	114

19	Heat Flux vs (T_{vap} - T_w) for Varying Thermal Resistances ----------	115
20	Effect of Air on Heat Transfer Coefficient During Dropwise Condensation --	116
21	Effect of Air on Heat Transfer During Dropwise Condensation ----------	117
22	Variation of Dropwise Condensation Heat Transfer Coefficient with Time -------	118
23	Heat Transfer Coefficient vs Heat Flux for Different Modes of Condensation -------	119
24	Heat Flux vs (T_{vap} - T_w) for Different Modes of Condensation ----------	120
25	Comparison of Experimental Data with the Condensing Curve as Proposed by Takeyama ----------	121
26	Variation of Dropwise Condensation Heat Transfer Coefficient with Surface Inclination ----------	122

LIST OF SYMBOLS

Symbol	Description	Units	
		Metric	English
A	Area	m^2	ft^2
c_p	Specific heat capacity	kJ/kg- °C	Btu/lbm- °F
d	Diameter	m	ft
g	Acceleration of gravity	m/sec^2	ft/sec^2
g_c	Gravitational constant	$kg-m/N-sec^2$	$lbm-ft/lbf-sec^2$
h	Local heat transfer coefficient	kW/m^2-K	$Btu/hr-ft^2-$ °R
$\bar{h}$	Average heat transfer coefficient	kW/m^2-K	$Btu/hr-ft^2-$ °R
h_{fg}	Latent heat of vaporization	J/kg	Btu/lbm
k	Thermal conductivity	W/m- °C	Btu/hr-ft- °R
L	Length	m	ft
m	Mass	kg	lbm
$\dot{m}$	Mass flow rate	kg/sec	lbm/sec
P	Pressure	kPa	lbf/in^2
q	Heat transfer rate	W	Btu/hr
q/A	Heat flux	W/m^2	$Btu/hr-ft^2$
r	Radius	m	ft
TC	Thermocouple reading	°C	°F
TQ	Quartz thermometer reading	°C	°F
T	Temperature	°C	°F
t	Thickness	m	ft

u	Velocity	m/sec	ft/sec
V	Volume	m^3	ft^3
x	Distance from leading edge	m	ft

Greek Symbols

α	Thermal diffusivity	m^2/hr	ft^2/hr
μ	Dynamic viscosity	kg/m-sec	lbm/ft-sec
ν	Kinematic viscosity	m^2/sec	ft^2/sec
ρ	Density	kg/m^3	lbm/ft^3

Subscripts

f	Evaluated at film conditions
L	Based on length of plate
s	Steam
ss	Steam side
sat	Evaluated at saturation conditions
vap	Evaluated at vapor conditions
w	Evaluated at wall
x	Denotes some local position with respect to x-coordinate

Dimensionless Groups

Nu_x	Local Nusselt number	$h_x x/k_f$
Nu_L	Average Nusselt number	$h_L L/k_f$
Pr	Prandtl number	ν/α
Re_x	Local Reynolds number	ux/ν

Conversions

Thermal conductivity:	1 kW/m-K = 577.8 Btu/hr-ft- °R
Heat transfer coefficient:	1 kW/m^2-K = 176.1 $Btu/hr-ft^2$- °R
Heat flux:	1 kW/m^2 = 317 $Btu/hr-ft^2$

ACKNOWLEDGMENTS

The author wishes to thank Mr. Ken Graham, the Naval Postgraduate School Chemist, who unselfishly contributed his time and expertise in glass blowing to build pieces of apparatus that would have taken weeks to procure and in chemistry to mix the chemical promoters.

Sincere thanks go to Professor Paul Marto, the author's thesis advisor, whose patience and knowledge provided the necessary guidance which brought this work to completion.

Lastly, but not least, the author wishes to express his thanks and appreciation to his wife, Frances, whose understanding and encouragement made the difficult times more endurable.

I. INTRODUCTION

The recovery of liquids is an extremely important aspect in a closed-loop cycle in which a liquid is boiled to produce a vapor to operate rotating machinery, such as turbines. The recovery is achieved through the process of condensation in which a vapor is allowed to come in contact with a surface whose temperature is maintained lower than the saturation temperature of the vapor at a given pressure. The removal of thermal energy from the vapor causes it to release its latent heat of vaporization, thus condensing onto the cooler surface. The condensate can form in two possible ways, either as a continuous film over the surface or as discrete drops. The method of condensation is determined by the ability of the condensate to wet the surface.

The presence of a liquid film over the condensing surface increases the resistance to the flow of heat from the vapor to the condenser surface. The thickness of the liquid film is determined by a balance between gravitational forces and viscous forces acting on the liquid. The temperature drop across this liquid film, due to the added resistance, causes a reduction in the amount of heat transferred through the condenser surface.

However, for the dropwise condensation process, the resistance to the flow of heat is negligible through the tiny drops as compared to the thicker liquid film. Without the added resistance of a film, the heat transferred through the condenser surface is therefore larger.

Filmwise condensation has received extensive analytical and experimental attention since the derived theoretical relations of Nusselt [1] in 1916. It has become a well-known process and thus has been used exclusively in the design of vapor condensers even though it is less efficient than the dropwise condensation process.

However, dropwise condensation is now receiving much attention in an attempt to reduce the size, weight, and cost of condensers. The reduction of size and weight is especially attractive to the enhancement of marine condensers.

A. DESCRIPTION OF THE CONDENSATION PROCESS

Consider what happens when a vertical flat plate is exposed to a condensable vapor, such as steam. If the temperature of the plate is below the saturation temperature of the vapor, condensate will form on the surface of the plate and will flow down the plate under the force of gravity. The process of condensation will either be in the filmwise mode or the dropwise mode. The two different modes of condensation are discussed below.

1. Filmwise Condensation

A simple theory of film condensation on a flat vertical plate was developed in 1916 by Nusselt [1]. The main features of Nusselt's theory were given qualitatively by Jakob [2] as follows:

Steam is condensing in a film on a vertical cooling surface. The film flows down, under the influence of gravity, but is retarded by the viscosity of the liquid. The heat of condensation passes through the film from the condensing steam to the wall. The film thereby resists the flow of heat; and therefore, a temperature drop exists across it. The temperature of the surface of the film in contact with the wall is equal to that of the wall, and the surface of the film in contact with the steam is assumed to be at the saturation temperature of the vapor. Also, it has been theorized that the film offers a strong resistance to the heat of condensation, which is conducted through it, and that the film becomes thicker as condensation proceeds, thus limiting its rate. However, to assume that the steam side of the film is always at saturation temperature and that the rate of condensation is dependent on the thickness of the film is not exactly valid. If the condensing steam is in contact only with a surface of liquid, and this is always at the saturation temperature, the vapor cannot know the

thickness of the liquid layer on which the rate of condensation is said to depend. Thus, the same mass would be condensed notwithstanding the thickness of the film.

Jakob [2] proposed the modification to Nusselt's assumption that the temperature of the liquid surface on the steam side of the film must be slightly lower than the saturation temperature and even lower with a colder cooling surface.

Quantitative analyses of the Nusselt theory are given by Jakob [2] and also by Holman [3]. From Holman [3], the local heat transfer coefficient (that is, the heat transfer coefficient at some distance x from the leading edge of the plate) is

$$h_x = \left[\frac{\rho_L(\rho_L - \rho_v)\, g\, h_{fg}\, k_L^3}{4\mu_L x(T_{sat} - T_w)}\right]^{0.25} \tag{1}$$

Introducing a dimensionless local Nusselt number

$$Nu_x = \frac{h_x\, x}{k_L}\,, \tag{2}$$

Equation (1) becomes

$$Nu_x = \left[\frac{\rho_L(\rho_L - \rho_v)\, g\, h_{fg}\, x^3}{4\,\mu_L\, k_L\, (T_{sat} - T_w)}\right]^{0.25}\,. \tag{3}$$

The average value of the heat transfer coefficient may be obtained by integrating over the length of the plate.

Therefore,

$$\bar{h} = \frac{1}{L} \int_0^L h_x \, dx = \frac{4}{3} h_{x=L} \tag{4}$$

and

$$Nu_L = \frac{\bar{h}L}{k} = 0.943 \left[\frac{\rho_L (\rho_L - \rho_v) \, g \, h_{fg} \, L^3}{\mu_L k_L (T_{sat} - T_w)} \right]^{0.25} \tag{5}$$

The fluid properties ρ_L, μ_L, k_L in the previous equations are the properties of the liquid condensate evaluated at the "film temperature",

$$T_f = \frac{T_{sat} + T_w}{2} \quad . \tag{6}$$

Several experimenters have questioned the assumptions made by Nusselt and have proposed various corrections to Equation (1). The reader is referred to Rohsenow [4], Bromley [5], and Gebhart [6] for the various corrections proposed.

The relation for the average heat transfer coefficient on a vertical plate from experimental data as recommended by Holman [3] is

$$Nu_L = \frac{\bar{h}L}{k} = 1.60 \left[\frac{\rho_L (\rho_L - \rho_v) \, g \, h_{fg} \, L^3}{4 \mu_L \, k_L \, (T_{sat} - T_w)} \right]^{0.25} \tag{7}$$

2. Dropwise Condensation

The phenomenon of dropwise condensation was discovered in 1930 by Schmidt, Schuring, and Sellschopp [7]. Although investigators of this phenomenon willingly accept the fact that large increases of the heat transfer coefficient occur in the presence of dropwise condensation, conflicting views have arisen concerning the mechanisms of dropwise condensation. The most popular theories proposed by investigators for the origination of drops have been based upon the existence of a thin film layer between the larger drops and the existence of nucleation sites on which the drops begin.

a. The Film Theory

Jakob [2] proposed this theory. The cooling surface was assumed to be covered by a very thin layer of water which continually and quickly grew in thickness until it fractured to form droplets. As the droplets coalesced and rolled off the surface, a portion of dry surface was exposed which was almost instantaneously covered by condensation of fresh steam so that the process repeated itself. Jakob claimed the high heat transfer coefficient was caused by the direct contact of the dry surface and the steam streaming to it.

Jakob's theory was supported by Baer and McKelvey [8] and Welch and Westwater [9]. In the latter work, high-speed motion pictures at speeds of about 4000 frames per second and a magnification of about 11x on the

negative indicated that the drops visible to the eye grew mainly by numerous coalescences which, upon forming, resulted in the vibration of the new drops that swept up the liquid film nearby. Thus it was concluded that condensation took place preferentially on the swept region and only slightly on the drops. The creation of this essentially "bare" surface between drops provided the explanation of the high heat-transfer coefficients obtained in the dropwise condensation process.

A somewhat similar view was proposed by Eucken [10], wherein an absorbed surface layer first forms and subsequently migrates into the base of neighboring drops. This mechanism has more recently been supported by Kast [11, 12]. Emmons [13] proposed a slightly different mechanism of dropwise condensation, that of re-evaporation in which vapor molecules condense momentarily on a bare surface between drops and give up thermal energy. The molecules then re-evaporate at a lower temperature and recondense on the drops.

b. The Nucleation Theory

An opposing view to the film theory was first presented in 1935 by Tammann and Boehme [14]. They observed that, upon repeated condensation, drops appeared to have the same arrangement on the condensing surface which suggested the existence of particular nucleation sites. Their observations have been subsequently supported

by other investigators: McCormick and Baer [15, 16], McCormick and Westwater [17], and Baer and Kontsky [18].

Umur and Griffith [19] used thermodynamic considerations and optical examinations of the condensing surface to conclude that no condensate film greater than a monolayer in thickness existed on the area between the drops. They proposed that no net condensation took place on the area between the drops; hence, nearly all the energy transferred to the cooling surface was transferred through the drops.

The nucleation theory has become the more generally accepted theory for drop growth, as illustrated by the many investigators, McCormick and Baer [16], LeFevre and Rose [20], Rose [21], Hurst [22], and Mikic [23], who have chosen the nucleation theory as their model of the dropwise condensation process.

c. Description of Dropwise Condensation

Dropwise condensation is a heterogeneous nucleation process. The nature of the heat transfer process is extremely complex due to its very transient behavior and non-uniformity over the condensing surface.

The phenomenon of dropwise condensation is described extremely well by Graham and Aerni [24] who follow the growth of a single drop from birth to departure.

The process is generally divided into four phases:

1) Nucleation. As the saturated vapor first encounters the condensing surface, it makes a phase transformation at discrete nucleation sites to form microscopic drops (approximately 0.5 micron in diameter). The nature of the surface must be hydrophobic (non-wetting), or the liquid condensate will form a film as opposed to droplets.

2) Condensation and Coalescence. In this phase, each of the microscopic droplets grows rapidly by direct condensation onto its surface. The drops continue to grow in size and occupy more surface area. Since there is a high density of drops on the surface, they begin to bump into one another and coalesce to form a larger drop. This larger drop continues to grow by condensation on its surface and by coalescing with its neighbors until it reaches approximately 0.1 mm in diameter. At this size, the drop can just be seen with the naked eye.

3) Coalescence. At the drop size just mentioned, conduction limitations cause the condensation to decrease radically. The resistance across the drop is so large that condensation of the vapor molecules on the drop surface no longer occurs. The large drop can now only grow through coalescence with smaller neighboring drops.

4) Departure. When the drop reaches a critical size, about 2 to 3 mm in diameter, the force of gravity overcomes the surface tension between the drop and the

condenser surface. In the case of a vertically oriented surface, the drop then slides down the surface, sweeping the area in its path. This swept area is larger than the diameter of the drop because of the oscillating motion of the drop as it progresses downward. This continuous sweeping by drops from the top of the condensing surface removes from the surface the larger drops which are nearly "inactive" to the condensation process, thus enhancing the heat transfer rate.

With the departure of a drop, one cycle of the process ends, and another cycle can begin on the bare area.

Through high-speed motion pictures, the time required for one cycle of dropwise condensation has been estimated to be on the order of milliseconds.

During the condensation process, the majority of heat transfer occurs through small "active" drops of less than 0.15 mm diameter. These drops make up only about 30 percent of the condenser surface; whereas the remainder of the surface is comprised of larger "dead" drops, greater than 0.15 mm diameter, and bare surface, about 60 percent and 10 percent respectively.

Even with the small percentage of effective condenser surface, heat transfer rates greater than 10 times that of filmwise condensation have been achieved.

3. Mixed Condensation

Whereas film and dropwise condensation are classified as "ideal" modes of condensation, there exists a

combination of the two modes which is so irregular as to prevent any analysis of its behavior. This form of condensation is called "mixed" condensation and is seen as smudged drops, streaks, and patches of continuous film. The heat transfer rates obtained for this mode of condensation are higher than total filmwise condensation but lower than pure dropwise condensation and are dependent upon the quantity of the two ideal modes.

B. A REVIEW OF DROPWISE CONDENSATION LITERATURE

During the past 45 years since the discovery of dropwise condensation, a multitude of experiments have been performed by numerous investigators to determine the magnitudes of heat transfer rates possible with this mode of condensation. The major problem encountered by experimental approaches to dropwise condensation has been the large number of parameters which can influence dropwise condensation. Graham [25] compares data from fifteen different experiments on the variation of heat transfer coefficient with heat flux. The range of the heat transfer coefficient is 5,000 to 70,000 Btu/hr-ft^2 - °F (28 to 400 kW/m^2 - K) for a heat flux range of near zero to 350,000 Btu/hr - ft^2 (near 0 to 1,100 kW/m^2).

The parameters that have been determined to date are:

1. Heat flux
2. Thickness of condenser surface
3. Pressure

4. Non-condensable gas concentration
5. Vapor velocity
6. Thermal conductivity of the condensing surface
7. Surface finish
8. Surface inclination
9. Location on the condensing surface
10. Condensing vapor
11. Promoter used
12. Vibration of the system
13. Condensate inundation

Graham [25] gives a detailed explanation of all of the above parameters except vibration of the system and inundation. This author will only present references on the particular parametric effects and conclusions from new work since Graham's work in 1972. Hurst and Olson [26] conducted an investigation involving dropwise condensation on thin copper foils in the horizontal orientation using a radiometer to measure the temperature gradient across selected drops. However, the investigation was limited by the finite diameter (0.8 mm) of the area measured by the radiometer and could not measure the temperature right under or just outside the perimeter of the drop. It was further limited by the problem of obtaining a reliable emissivity on the cooled side of the test surface.

In conjunction with the experimental runs the authors [26] presented a finite-element analysis of the drop and

condensing surface. From their experiment and analysis, the authors concluded that a condensing surface should be able to diffuse laterally the concentrated heat source from a drop so that heat could be transferred out of the condensing surface across a comparatively high heat transfer resistance into the coolant stream. They compared this diffusion to a fin in a forced-convection situation. Their conclusion implied that there must be some sort of minimum condensing-wall thickness below which its function as a fin cannot be efficiently carried out.

Pressure

Wilmshurst and Rose [27] condensed steam on two copper condensing surfaces, one promoted with dioctadecyl disulphide and the other promoted with a thin layer of polytetrafluorethylene (ptfe), to show the influence of pressure on heat transfer during dropwise condensation. Their conclusions for the chemically promoted surface at subatmospheric pressures were that the heat transfer coefficient increased as the heat flux increased, with constant pressure; and the heat transfer coefficient decreased with a decrease in pressure, with constant heat flux. Their results at near-atmospheric conditions showed a larger heat transfer coefficient for higher heat flux.

Thermal Properties of the Condensing Surface

Nijagura and Abdelmessih [28] and Hannemann and Mikic [29] wrote papers that show, theoretically, that the heat transfer coefficient increases as the thermal conductivity

of the condenser surface increases. Hannemann and Mikic [30] in a companion paper to the one above [29], ran an investigation to compare experimental data to the results of their theoretical analysis. Agreement between the two and to other works was considered to be good. However, experimental work carried out by Aksan and Rose [31] on identical copper-plated mild steel and copper surfaces disagrees with the above conclusions. Their results for heat fluxes in the range of 200 to 370 kW/m^2 show no significant effect of the thermal properties of the condensing surface materials.

Surface Finish

Recent work by Abdelmessih, Neumann, and Yang [32] using gold plated copper condensers emphasized the fact that smooth condenser surfaces provided higher heat transfer coefficients than rough surfaces.

Surface Inclination

Citakoglu and Rose [33] performed an investigation of the effect of surface inclination on the dropwise condensation heat transfer coefficient for the range of 5 to 180 degrees (face down) at 10 degree intervals. Their results indicated a dependence on the surface inclination but only after tilting the surface more than 60 degrees in either direction from vertical. Citakoglu and Rose also reported the appearance of a second maximum for the heat transfer coefficient at about 140 degrees, but it was

less than the one at 90 degrees and was most pronounced at higher heat fluxes.

Tanasawa, Tachibana, and Ochiai [34] provided a 3-part report which consisted of a digital computer method for simulating the entire process of dropwise condensation, an investigation of the process of drop growth due to condensation of vapor onto the drop and by coalescence with neighboring droplets, and an experiment to provide data to check the digital method. Among their experimental observations was the effect of surface inclination between the angles of 15 and 150 degrees. Their results for inclination are similar to previous investigators, except that they did not observe the double maximum value as reported by Citakoglu and Rose [33].

Location on the Condensing Surface

No evidence of heat transfer coefficient dependence on plate height was found in the work by Le Fevre and Rose [35] for vertical copper condensing surfaces of 25.4 to 101.6 mm (1 to 4 in.). However, in a more recent paper by Rose [36], he concluded that the heat transfer coefficient actually increased with distance down the surface. He gave three factors for this increase:

1. Coverage by falling drops is in general small, and variations with height have correspondingly small effect on the heat transfer coefficient.

2. Decreased coverage due to growth of falling drops as they proceed down the surface is counteracted

by the fact that the falling drops accelerate and consequently become more widely spaced. Alternatively, a falling drop may, despite its increase in size, cover a lower region for a shorter time than it does a higher region.

3. Since falling drops grow as they proceed down the surface, they sweep diverging tracks. Consequently, lower regions are swept more frequently.

Condensing Vapor

As stated by Graham [25], several experiments have been conducted utilizing different condensing vapors, but no comparison could be made due to the use of different apparatus. However, one investigation of dropwise condensation by Kirby [37] was carried out for ethyl alcohol, methyl alcohol, and acetone on a polytetrafluorethylene coated iron tube and compared to filmwise condensation of the same vapors on a bare iron tube. The increase of overall heat transfer coefficient of dropwise over filmwise was 30, 45, and 65 percent respectively for the vapors mentioned above.

Promoter

Substances which promote surfaces for dropwise condensation have been studied extensively in recent years. Promoting a surface to make it non-wetting to the condensate is necessary for all condenser materials, with the possible exception of the noble metals.

There are four categories of promoters: 1) chemically adhering, 2) physically adhering, 3) non-adhering, and 4) noble metals. Of these four, the areas of most investigations are the chemically adhering and physically adhering promoters. However some work is being done to plate surfaces with thin layers of noble metals. This method of promoting surfaces for dropwise condensation has been studied in the works of Erb [38,39] and Erb and Thelen [40].

Studies using tetrafluoroethylene (teflon) and polytetrafluoroethylene coatings have been made by Kirby [37], Davies and Ponter [41], and Ponter and Diah [42]. The problem to date using this promoter is getting an extremely thin layer on the surface and finding the ideal thickness. Should too thick a layer be put on the surface, the insulation properties reduce the effectiveness of dropwise condensation down to and below that of filmwise condensation. However, new techniques of vapor deposition are being studied which can control the thickness deposited down to a monolayer of the promoter material.

Chemical promoters have received a large amount of attention because of their ease of application. They can be sprayed on, brushed on, or injected into the condensing vapor. The disadvantages of chemical promoters are the unknown effects to steam boilers and other components, their relative short life as compared to the permanent

promoters, handling difficulties, and the need for different chemicals for different condensing surfaces.

The primary objective of research of chemical promoters is to find a combination that will strongly adhere to the condenser surface and also will remain non-wetting to the condensing vapor. Extensive work has been carried out by different investigators [43,44,45,46,47,48,49,50] on different promoting chemicals. A summary of some dropwise promoters and their characteristics is given in Fox [51].

The last two parametric effects will become increasingly important as experimenters move from single tube and flat plate condensing surfaces to larger and multi-tube condensers. Previous experiments have concentrated, and rightly so, on becoming familiar with the dropwise condensation phenomena before attempting a specific application.

There has been very little investigation on the effects of vibration on dropwise condensation. Graham [25] was able to take a limited amount of data prior to the burn out of his "shaker", which indicated a slight increase in the heat transfer coefficient with increased vibration. The reason for the increase in the heat transfer coefficient is that the vibrating motion helps overcome the surface tension between the large "inactive" drops and the condensing surface. This would serve a two-fold purpose: 1) It would cause the surface to be swept more frequently,

and 2) it would remove the "inactive" drops from the surface, thus allowing more conduction to occur through the smaller "active" drops.

The effect of inundation of lower tubes by condensate dripping from the top tubes in a condenser must be investigated fully to determine the limiting rate of condensation. If the rate of condensation becomes great enough, the lower tubes of a large condenser could become flooded with condensate and cause a substantial decrease in the heat transfer rate. Watson, Brunt, and Birt [46] concluded that the effect of inundation may be ignored for tube bundles of less than 40 rows high. Other views on inundation are presented in the literature [52,53,54].

C. OBJECTIVES OF THIS WORK

The objectives of this study are:

1. To study the temperature pattern of thin condensing surfaces experiencing dropwise condensation using cholesteric liquid crystals. This method of observing temperature changes has been used successfully on thin foils experiencing nucleate boiling [55]. Since dropwise condensation is considered to be a nucleation process, it was believed that liquid crystals would reflect the temperature patterns of the thin foil.

2. To become more familiar with the dropwise condensation phenomenon, the operating procedures to obtain dropwise condensation, and the factors which influence dropwise condensation.

3. To study the effects of inclination on the heat transfer rate during dropwise condensation.

4. To record any other factors observed while utilizing the dropwise condensation mode.

II. DESCRIPTION OF EXPERIMENTAL APPARATUS

The objective of this work is to study dropwise condensation on flat condensing surfaces in different orientations. Figure 1 shows a schematic diagram of how the experimental apparatus was situated to achieve the objective. Figure 2 presents the entire apparatus arrangement in a photograph.

The apparatus consists of three major components: 1) the boiler section, 2) the condenser section plus the various test surfaces, and 3) the instrumentation.

A. STEAM SYSTEM COMPONENTS

1. Boiler Section

The boiler section consisted of a stainless steel boiling vessel resting upon a 1000 watt, 120 volt a.c. hot plate. The cylindrical boiling vessel was fitted with a flange in which an "0" Ring groove had been machined. When the top was placed on the "0" Ring and clamped with C-clamps, an air tight seal was achieved. The capacity of the boiling vessel was 13.5 liters of distilled water which provided approximately 12 hours of boiling time at a maximum steam flow rate of 1.59 kilograms per hour (3.5 pounds per hour).

Stainless steel was chosen for the material to preclude contamination of the steam and to allow safe operation under sub-atmospheric conditions.

The boiler was connected to the piping system by a brass joint shown in Figure 3, which was tapered to fit into a matching taper in the boiler top. An "0" Ring installed in the middle of the taper of the joint provided an airtight seal between the boiler and the joint.

The opposite end of the joint was machined straight so that it would fit into a pressure coupling. This connection allowed the operator to remove the boiler top without disturbing the rest of the system. When the pressure coupling was tightened, an "0" Ring made the seal between the joint and the steam piping.

In the joint (See Figure 3.) was soldered a steam control petcock valve. The purpose of this valve was to regulate the steam flow from the boiler. Air leaks were prevented from entering through this valve by two "0" Rings on either side of the opening.

2. Steam Ejection System

To obtain sub-atmospheric pressures in the condenser test section, a single stage air ejector was used. The air ejector, purchased from Graham Industries, was specifically designed for laboratory use and is motivated by compressed air at 791 kPa (100 psig).

Subsequent to the purchase of the air ejector, it was modified for use in another project by removing the converging-diverging nozzle and replacing the nozzle with a section of straight 19 mm diameter pipe. Although the performance of the ejector is degraded, system pressures

of less than 34.5 kPa (5 psia) were obtainable with the present arrangement. This pressure was considered more than adequate for the present objectives.

The ejector operation is still basically the same as before the modification was made. Air enters a converging nozzle. As the air travels through the nozzle, it increases in velocity until it dumps into the entrance of the diffuser section. As it travels through the diffuser, it entrains the surrounding vapor and carries it out through the diffuser exit.

The condenser test section can be evacuated by connecting the exit piping of the condenser to the diffuser section of the air ejector.

The system pressure can be regulated through the use of a throttling valve on the compressed air inlet of the ejector.

B. CONDENSER TEST SECTION

The condenser test section was designed by Moreno [56]. The condenser test section in the present arrangement is composed of: the Condensing Chamber, Baffle Housings, End Caps, Observation Port, Illumination Port, Pressure Couplings, Condensing Chamber Insert and Clamps, and Cooling Water Director. Figures 4 through 10 show the details of each component. Figure 11 shows a close-up photograph of the Condenser Test Section.

1. Condensing Chamber

The condensing chamber was built from stainless steel plates 6.35 mm thick with cut-outs located in the front, top and back plates. Figure 4 shows the dimensions and shape of the chamber. The chamber was designed to be an air tight chamber with welded construction and bolted joints utilizing "0" Ring gaskets. The front cut-out, 76.2 mm by 76.2 mm, was for observational and photographic purposes; and the top cut-out, 139.7 mm by 60.5 mm, was for illuminating inside the condensing chamber. The back cut-out, 52.4 mm by 52.4 mm, was for the insertion of the original test surface. Four holes were originally drilled in the back of the chamber, but for the present work only one was utilized for connecting the chamber to a Mercury manometer. The other three holes were plugged using bolts covered with teflon tape to seal the threads for the two smaller ones and a plug utilizing an "0" Ring seal for the larger ones. A condensate drain was installed in the bottom of the chamber to drain off the condensate as it condensed on the test surface.

To facilitate the present work, the following modifications were made to the condensing chamber:

a. Three holes on the back side were plugged as described above.

b. Two holes were drilled in the bottom on the axial centerline for installation of thermocouples to measure the vapor temperature inside the chamber.

c. The previous condensate drain was enlarged.

d. The gasket groove on the back plate around cut-out was enlarged to 6.35 mm wide by 1.59 mm deep.

2. Baffle Housings

A stainless steel baffle housing containing stainless steel, grid-type baffles was installed on each end of the condensing chamber to direct the steam flow in uniform streams over the test surface. This was an attempt to provide a straight through steam path which would eliminate stagnant flow and a concentration of non-condensable gases. The baffle housings were constructed of the same 6.35 mm stainless steel as the condensing chamber. They were bolted to the condensing chamber and sealed with "0" Ring gaskets placed in grooves machined in the flanges of the baffle housings. Figure 5 shows the details of these housings.

3. End Caps

Two end caps made of 6.35 mm thick stainless steel plates were bolted and sealed to the baffle housings in the same manner as the baffle housings were connected to the condensing chamber. Figure 6 shows the details of the end caps. The purpose of the end caps was to prevent stagnant vapor concentration in "dead pockets" at the inlet and outlet of the condensing chamber as a result of

sharp corner connections between plates. Also the shape of the end cap was an important factor to prevent dead air spaces.

4. Observation Port

Two 90.5 mm by 90.5 mm by 6.35 mm plates of Borosilicate glass 7740 (Pyrex brand) were used to build up the observation port. It was constructed of an aluminum frame and a 6.35 mm thick piece of sheet rubber, which was cut to fit in the frame and separate the glass. Holes were drilled in the rubber to allow hot air to pass through the formed chest between the glass to minimize condensation on the glass. Figure 7 shows the details of this port.

The assembly was then attached to the side of the condensing chamber with studs through the corners of the frame. An "0" ring groove machined in the condensing chamber held the "0" ring between the chamber and the inside piece of glass to effect an air seal.

5. Illumination Port

The illumination port served as a light source in the original design of the Condenser Test Section. However, it served no use in the present work because the insert, needed to hold the test surface, blocked any light from this port to the surface. Because of this, the test surface had to be illuminated through the observation port.

6. Condensing Chamber Insert and Clamps

The cut-out in the back plate of the condensing chamber was too large for use with the test surface of the present work. The modification chosen was to manufacture an insert which would fit into the existing cut-out and also would hold the test surfaces. Figure 8 shows this insert. A rubber gasket was used to seal the step of the insert against the condensing chamber. The insert was designed so that the inside of the insert would align with the inside of the condensing chamber. The steamside edges of the insert around the test surface were bevelled to allow an unobstructed steam flow path to the test surface and to prevent a build up of condensate on the bottom of the test surface.

The insert was held against the condensing chamber by a clamp over the outer edges of the insert. Slots were machined on two faces of the clamp to prevent interference with the cooling water director (discussed in the next section).

7. Cooling Water Director

The purpose of the cooling water director was to direct a measured quantity of tap water over the water side of the test surface and out to the drain line. The water director was machined in two pieces and soldered together to form the assembly shown in Figure 9. Solid rectangular channels were soldered to this assembly to

reduce the flow channel to 6.35 mm O.D. copper tubing. Brass was chosen as the material for the water flow director because of its ease of machining over stainless steel.

Slots were used as the inlet/outlet to allow maximum water flow through the director and still retain enough strength to allow clamping without bending the director. The slots were positioned so that no stagnant water pockets existed.

Sheet rubber gaskets were placed on either side of the water director to prevent water leakage between the water director and the test surface on one side and the Plexiglas sight glass on the other side.

A clamp was placed on the studs in the insert, and nuts were used to tighten the clamp down on the components of the cooling water side.

The inside edges were bevelled on all sides to allow maximum viewing of the back side of the test surface when liquid crystals were used for temperature measurement since the liquid crystals must be photographed at an incidence angle of approximately 30 degrees.

8. Pressure Couplings

A pressure coupling was silver soldered to each End Cap of the condenser test section. With this coupling loosened, the entire condenser test section could be tilted to different angles of inclination. Tightening

the coupling caused a seal between the "0" ring gasket and the stainless steel piping. Figure 10 shows the arrangement of the coupling.

9. Test Surfaces

During the present work, the following test surfaces were used:

a. 3.175 mm (1/8 inch) thick copper plate
b. 0.051 mm (0.002 inch) thick copper foil
c. 0.051 mm (0.002 inch) thick copper foil with Mylar epoxied to the back side
d. 0.0051 mm (0.002 inch) thick titanium foil, commercial grade Type A-75.

All of the copper surfaces were of high purity composition.

The test surfaces, cut to a square with outside dimensions of 38.1 mm by 38.1 mm, were fitted into the recess of the insert. The actual surface area available for condensation was 645.2 mm^2 (25.4 mm by 25.4 mm). Thermocouples were soldered on the back side of the copper surfaces and were tack welded on the back side of the titanium foil. Figure 12 shows the size of the test surface and the general arrangement of the thermocouples although the attachment procedures were different for each surface. These procedures are presented in Appendix A. Since no attempt was made to determine temperature variations over the plate, but only to determine an average

surface temperature, the exact location of each thermocouple was not determined.

C. INSTRUMENTATION

Accurate heat transfer measurements are very important when investigating both filmwise and dropwise condensation. However, since the temperature difference between the saturated vapor and condensing surface is much smaller for dropwise condensation, the effect of inaccuracies in temperature becomes more pronounced. Thus an effort was made to utilize the most accurate measuring instruments in a manner most likely to produce reliable results.

The measuring instruments used in this thesis are discussed in the following paragraphs.

1. Temperature Measurement System

a. Thermocouples

Due to the thickness of the test surfaces, one-dimensional heat flux was assumed which made accurate measurement of the surface temperature a necessity. To obtain this accuracy the thermocouples were attached carefully to the surface. The goal was to ensure that the thermocouple bead was in good contact with the water side surface. Appendix A lists in detail the procedures used to attach thermocouples to the surfaces.

Five thermocouples, TC6 through TC10 were attached to each test surface as shown in Figure 12. Each thermocouple was made of 0.127 mm (0.005 in) Copper-Constantan wires which were insulated with a Teflon coating.

First the junction was made by welding the wires together using a Dynatech Model 116SRL Tungsten Inert Gas Thermocouple Welder, using Argon gas to provide the inert atmosphere. The combination of the tungsten, with a low burn-off rate, and the argon atmosphere around the weld area provides a stronger and more reliable weld than ordinary pressure welding. The oxide contamination is reduced which enhances the accuracy of the thermocouple.

The thermocouple bead was then flattened to provide more contact area between the test surface and the bead. The thermocouple leads were soldered to Copper-Constantan extension leads which were connected to a Newport Model 267 Digital Pyrometer.

The Newport Digital Pyrometer is an instrument which senses the voltage from the thermocouple bead, performs an analog linearization operation on the signal, and, using a dual slope technique, converts the signal to a digital display which is read by the experimenter directly as degrees celsius. The instrument uses a precalibrated bipolar signal integration around zero which eliminates the need of an ice reference.

Using Copper-Constantan sensor material with Copper-Constantan thermocouples at an ambient temperature of 25 °C gives a resolution of 0.2 °C and an overall error of ± 0.2 °C for this thermocouple system. The author felt these error limits were tolerable for the present work.

The vapor temperature was measured with two 0.25 mm diameter (30 gauge) Copper-Constantan thermocouples, TC11 and TC12, located at the inlet and outlet and on the centerline of the condensing chamber. The thermocouple probes were located in the chamber such that each thermocouple was directly exposed to the steam as it entered and exited the condensing chamber. These thermocouples were read through the Newport Pyrometer, and their average value gave the vapor temperature in the chamber. The maximum difference between these two temperatures was 0.2 °C.

There were two 0.25 mm diameter (30 gauge) Copper-Constantan thermocouples TC15 and TC16, in the cooling water inlet and outlet lines which also were read on the Digital Pyrometer. These thermocouples served only as a check for the cooling water temperature difference across the test surface and were not used in heat transfer calculations, although they had the same accuracy as those thermocouples used in the vapor chamber.

Two other thermocouples, TC13 and TC14, of the same materials and connected in the same manner as the vapor temperature and cooling water difference thermocouples, were used to regulate the temperature of the hot air into the windows of the condensing chamber and to serve as a warning device should the boiler run low on water.

All of the temperature measuring instruments were calibrated at one time using a variable temperature oil bath following the steps of Appendix B.

An additional output display for the thermocouples was the Brush Mark 280 Recorder. The selected thermocouple lead was connected to a junction which carried the thermocouple signal through a high gain D.C. preamplifier to the Brush recorder. The signal was converted to millivolts and recorded on moving chart paper.

With system inaccuracies of 0.5 percent and response times of less than two milliseconds, the Brush recorder can show very precisely the temperature changes at a point on the test surface for any time period.

Recordings were obtained for all test surfaces under different test conditions. Appendix C gives the steps taken to record and interpret the data obtained for a particular operation.

b. Quartz Crystal Thermometers

Since the temperature difference of the cooling water across the test surface was expected to be small, especially at high cooling water flow rates, a more accurate system of measuring these temperatures was desired. The system that was adequate and available was a Hewlett-Packard Model 2801A Quartz Thermometer. This thermometer indicates temperature as a consequence of

frequency changes exhibited by temperature sensitive quartz crystals used as sensing elements. The quartz crystals are hermetically sealed in cylindrical stainless steel cases in a helium atmosphere. These probes were installed in holders, and the cooling water was passed over them. The direction of water flow onto this quartz crystal thermometer was arranged so that good mixing occurred over the probe and a time bulk temperature of the cooling water was measured.

The inlet thermometer was designated TQ1, and the outlet thermometer was designated TQ2. The signal is transported to the parent instrument through flexible coaxial cable. The parent instrument which also contains the digital display performs an integration on the signal, providing an average value of the probe temperature over a fixed reading time. For the 0.0001 °C resolution selected for the present work, a sample time of one second was used.

The calibration accuracy of the probe-thermometer combination at the factory was to within 0.02 °C. The quartz crystal thermometers were calibrated prior to use in this experiment in the variable temperature oil bath using the procedures given in Appendix B.

c. Liquid Crystals

Liquid crystals were first observed in 1888 by the Austrian botanist Friedrich Reinitzer but never attracted much interest in liquid-crystal research due

to the apparent lack of practical applications [57]. However, beginning in 1958, Fergason [57] and his colleagues began a research project to learn more about liquid crystals. They found liquid crystals could be used successfully in thermal mapping because the crystals responded to different temperatures by changing colors. Fergason [58] later did further research using liquid crystals in nondestructive testing.

In the last five years, liquid crystals have been used successfully as temperature sensing devices by Raad and Myers [59]; Smith, Gisser, Young, and Powers [60]; and Cooper, Field, and Meyer [61]. Other uses of liquid crystals have been explored. Some of this work can be found in references [62,63,64].

In the works of Rivers [55] and Raad and Myers [59] cholesteric phase liquid crystals were used to measure the temperature fluctuations on the surface of thin foils undergoing nucleate boiling. Due to the thinness of the foil, temperature fluctuations on the upper (boiling) surface around the nucleation sites produced corresponding variations on the underside of the foil causing color changes of the liquid crystals [59].

The motivating factors for using liquid crystals in the present study were the results obtained by Hurst and Olson [26] and Detz and Vermesh [65] for

dropwise condensation. They both stated that the temperature is not constant under a drop during dropwise condensation, but rather the surface temperature increased as the edge of the drop was approached from the inner part of the drop.

Since it is not possible to place thermocouples on the condenser surface to record the temperature gradient under individual drops, liquid crystals were tried. And since dropwise condensation has been described as a nucleation process, it was thought that liquid crystals would give similar results as obtained by the two previously mentioned works.

The procedure for applying the liquid crystals is duscussed in Section A.3 of Chapter III, Experimental Procedures.

Liquid crystals have a resolution quality of 20 line pairs per millimeter and a speed of response of less than 0.2 seconds [66]. These characteristics are very favorable for use with the dropwise condensation process. Simultaneous photographs were to be taken of each side of the condensing surface to permit analysis of the drop distribution on the condensing side and the temperature pattern on the back side of the foil.

However, the use of liquid crystals was abandoned due to difficulties encountered. These difficulties are discussed in Section A of Chapter IV, Presentation and Discussion of Results.

2. Flowmeter

Tap water was used to cool the back side of the test surface. The flow of water over the test surface was regulated by a Fischer and Porter Precision Bore Flowrator, Model 10A3565A, Tube No. FP-1/2-27-G-10/83, with a maximum flow rate of 0.070 kg/s (0.155 lbm/s) of liquid with a specific gravity of 1.0. Appendix B gives the procedures used to calibrate the flowmeter.

Figures 1 and 2 show the location of the flowmeter in the apparatus arrangement.

3. Mercury Manometer

In order to measure the pressure inside the condensing chamber, a vacuum hose was connected from a hole in the back plate of the chamber to a U-tube mercury manometer, which was marked off in millimeters. The location of the manometer can be seen in Figures 1 and 2.

D. PHOTOGRAPHIC EQUIPMENT

High speed motion pictures were taken through the observation port of the condensing chamber, using a Fairchild Model HS401 Motion Analysis Camera. The camera was capable of speeds up to 8000 frames per second; however, speeds of 160, 600, and 920 frames per second were used during this experiment. The different speeds were achieved by utilizing one of four interchangable drive motors and varying the voltage input to the motor for a particular speed range.

Power to the camera was supplied by a Fairchild Model HS-5101B Motor Control. A 30 amp, 115 volt AC source provided sufficient current to operate the rectifier in the Motor Control. An output range of 9 to 40 volts DC was supplied to the Motion Analysis Camera.

The camera was mounted on a Fairchild Model HS-2511 tripod for film runs when the test surface was in the vertical position and was bolted to a wooden camera stand, which had been affixed to the laboratory table, for runs when the test surface was in the horizontal position.

The lens system was constructed from the optical portion of a Gaertner optical strain gauge readout system. A bayonet lens mount was machined, and the lens was mounted on the camera. This lens gave a magnification of 20X.

Since the lens system used was not a commercially furnished lens, a different focusng technique had to be adopted. First, a roll of unexposed film on which felt-tip pen marks had been made on the emulsion side was loaded into the camera. The marks were aligned opposite the view finder. The boroscope was focused on these marks. The camera was then positioned so that the best image focused on the film. The boroscope was removed, and the camera was run.

Lighting was provided on the subject by a Color-Tran Multi-6 light fixture, Model No. 100-071, with a 650 watt,

very narrow spotlight placed approximately 300 mm from the surface to be photographed.

Kodak 2475 Recording Film (ESTAR-AH Base) was used for the experimental runs. The film was processed commercially using normal processing procedures.

III. EXPERIMENTAL PROCEDURES

A. TEST SURFACE

1. For Filmwise Mode

For any surface to condense in the filmwise mode, it must be absolutely free of organic contamination. Should any organic materials be on the surface or in the steam, the surface will condense in the dropwise or mixed mode.

Copper surfaces used in this experiment had not been exposed previously to any commercially prepared dropwise promoter and were thus cleaned in a manner to remove greases and cutting oils which may have come in contact with the surface during handling and cutting operations. Bromley, Porter, and Read [47] give a more drastic cleaning procedure to be used with surfaces exposed to dropwise promoters.

The copper and titanium foils were used in the "as received" condition. The copper plate was cut to size and polished to a near mirror finish using a technique similar to Graham's [25] by rubbing it on a matallurgical polishing cloth soaked first with 0.3 micron and then 0.05 micron aluminum oxide polishing compound.

It was believed that all the surfaces were at nearly the same finish by the time thermocouples were installed and the surface handled.

The copper surface was first dipped in a 50 percent solution of hydrochloric acid to remove any oxides which may have formed on the surface and then rinsed thoroughly with distilled water. Next, it was cleaned with a wetting procedure adapted from Tucker [67] as follows:

1. Scrub the surface with a bristle brush and a chlorinated hydrocarbon degreasing compound such as trichloroethane. (Avoid prolonged breathing of the vapors.)

2. Rinse with distilled water.

3. Scrub foil with a mixture of equal parts of 50 percent sodium hydroxide solution and ethyl alcohol, warmed to approximately 85 °C, again using a bristle brush.

4. Rinse with distilled water.

5. Scrub foil with a 10 percent sulfuric acid solution at room temperature.

6. Rinse several times with distilled water.

7. Allow to dry.

Filmwise condensation was not attempted on the titanium foil.

2. <u>For Dropwise Mode</u>

The promoter selected for use in this work was a mixture of one percent by weight of n-octadecyl mercaptan (or octadecanethiol, $CH_3(CH_2)_{17}SH$) in octanoic acid (or caprylic acid, $CH_3(CH_2)_6CO_2H$). This compound was found

to be an excellent promoter, second only to tetrakis octadecyl thio silane ($(C_{18}H_{37}S)_4Si$), by Bromley, Porter, and Read [47]; Wilkins, Bromley, and Read [48]; and Bromley and Read [50]. Several attempts made by the author to acquire the tetrakis octadecyl thio silane were unsuccessf[illegible].

The octadecyl mercaptan was found by the above researchers to produce 100 percent dropwise condensation for a period of 3 to 5 weeks. These two aspects exceeded the requirements of a good promoter for the present work.

The procedure for applying the promoter to the copper surface was:

1. The surface was swabbed with a 50 percent solution of hydrochloric acid to remove any oxide that may have formed on the surface.

2. It was then rinsed thoroughly with distilled water. Excess water was removed.

3. The condensing surface was wiped, ensuring complete coverage, with a cotton swab saturated in the promoter mixture.

4. Excess promoter was rinsed off the surface with distilled water.

5. The test surface was immediately installed in position in the condensing chamber, and the cooling water was turned on. This step was done with the temperature inside the condensing chamber at the saturation

temperature of the vapor. Dropwise condensation began immediately on the condenser surface.

3. Application of Liquid Crystals

The liquid crystals were supplied from the manufacturer in encapsulated form, that is, with a protection coating around the crystals.

The procedures for cleaning the surface and applying the liquid crystals were:

1. The copper foil was dipped in a 50 percent solution of hydrochloric acid to remove any oxide from the surface.

2. The surface was cleaned with acetone, to remove any greases and fingerprints and was then dried.

3. The surface was sprayed with Testors No. 1249 flat black spray paint to provide the proper background for the liquid crystals.

4. The liquid crystals were sprayed onto the black paint with a compressed-air-powered air brush held about one-half meter away from the surface. Eight to ten coats of liquid crystals were sprayed on, which gave a coating of liquid crystals of about 0.03 mm thick. An electric heat gun was used between coats to dry the previous layer and expedite the operation.

Since the liquid crystals are water soluble, some means had to be provided to protect them from the cooling water which cooled the back side of the foil during the

condensation process. An additional requirement of the protection was that it should not interfere with the observation of the color changes of the liquid crystals. Many experiments were made by the author to find a suitable protection. A coating or covering installed over the liquid crystals was decided to be the best method. In this case, the liquid crystals were coated with 5-minute epoxy glue and then covered with a piece of 0.025 mm thick Mylar foil which was pressed in the glue until all air bubbles were removed. The foil was pressed between two metal plates to ensure good adhesion of the components. A brass ring was glued over the Mylar to prevent water from getting under the edge and on the liquid crystals.

B. HEAT TRANSFER DATA REDUCTION PROCEDURES

Since the heat flux was mainly controlled by the amount of tap water flowing over the back side of the test surface, it was decided for each experimental run to vary the mass flow rate of water through five different flow-rator levels ranging from 20 to 100 percent flow. The steam pressure was kept constant at atmospheric pressure, and the steam velocity remained the same throughout the experimental runs.

1. Heat Flux Determination

The heat flux through the condensing surface was obtained using the equation

$$q/A = \frac{\dot{m}_{cw} c_p \Delta T_{cw}}{A} \quad (8)$$

where

$\dot{m}_{cw}$ = cooling water mass rate of flow from flowmeter (kg/s)

c_p = specific heat of the cooling water at the average temperature (kJ/kg - °C)

ΔT_{cw} = cooling water temperature difference from quartz crystal thermometers (°C)

A = surface area of the condenser surface (m^2).

2. Temperature Determination

The temperature of the water side of the condensing surface was obtained by reading the value of the five thermocouple outputs through the Newport Digital Pyrometer in degrees celsius. An arithmetic average of these temperatures was taken, and the correction factor from Table 1 was applied to it. The vapor temperature was measured by two thermocouples located at the inlet and outlet of the condensing chamber. Their readings were averaged, and the appropriate correction factor from Table 1 was applied.

The temperature difference of the cooling water was obtained by first recording the values of the two quartz crystal thermometers and applying their respective corrections from Table 2 to each reading. Then their arithmetic difference was taken.

The other thermocouple temperature measurements were used only as checks and to ensure safe operating conditions of the boiler. Their values were not used in the heat transfer analysis.

The steam-side temperature of the test surface was obtained by first using the heat flux, as calculated above, and the Fourier heat rate equation to obtain the change in temperature across the test surface, ΔT_w. This temperature change through the plate was then added to the water side temperature, from above.

Knowing the heat flux and the vapor and surface temperature, the heat transfer coefficient can be computed using Newton's Law of Cooling.

3. Steam Velocity Determination

The velocity of the steam vapor through the condensing chamber was obtained by using the relationship between the heat transfer rate and the mass rate of flow. Assuming saturated steam from the boiler,

$$q = \dot{m}_s h_{fg} = \rho_s A V_s h_{fg} \qquad (9)$$

where

q = output of the boiler (watts)

$\dot{m}_s$ = steam mass rate of flow (kg/s)

h_{fg} = heat of vaporization (J/kg)

ρ_s = steam density (kg/m^3)

A = cross-sectional flow area of condensing chamber (m^2)

V_s = velocity of steam (m/s).

Note that this relationship will give the maximum steam velocity due to the assumption of no losses in boiler efficiency.

4. Steady State Determination

Although the test surface was rinsed with distilled water after the promoter was swabbed onto the surface, it was believed that there was still an overabundance of promoter on the surface. This extra promoter constitutes an additional resistance to the heat transfer process and can cause erroneous readings. After some time of condensing on the surface, the measured heat-transfer coefficient will reach a steady value. Except for Run 2, all data for heat measurements was taken at least three hours after condensation began on a newly promoted surface. The time for Run 2 was 1 1/2 hours. The transient behavior caused by the promoter is explained more fully in the next chapter.

5. Photographic Procedure

After all heat transfer data had been recorded, photographs were taken of the 3.18 mm (0.125 in) thick copper plate undergoing dropwise condensation for both the vertical and horizontal (face down) orientations. Figures 13 and 14 show the typical results obtained.

In order to get a better understanding of the dropwise condensation phenomenon, high speed motion pictures were taken through a microscopic lens which gave a magnification of about 20X. Again both vertical and horizontal (face down) orientation were recorded.

IV. PRESENTATION AND DISCUSSION OF RESULTS

A. GENERAL

There was a total of eight experimental runs made in which the data was reduced and used for the results of the present work. In addition to the runs above in which thermocouples were used for temperature measurement, several runs using liquid crystals for temperature measurement were made. Table 3 shows the details of the eight data runs and two representative runs using liquid crystals. The parametric effects of heat flux, non-condensable gas, promoter, condensing surface thermal properties, and condenser surface inclination were investigated during dropwise condensation. The performance as a result of these parameters was compared through the data presented.

B. QUALITATIVE OBSERVATIONS

Some of the results of this work could not be reduced into data but served as a means for the author to become more acquainted with the mechanisms of dropwise condensation. These observations were made through the use of liquid crystals, high-speed motion and still pictures, and the Brush recorder temperature traces.

1. Liquid Crystals

Many attempts were made to use liquid crystals on the coolant side of the 0.13 mm (0.005 in) and the

0.05 mm (0.002 in) thick copper foils to show the condenser surface temperature distribution while the condenser surface was undergoing dropwise condensation. Encapsulated liquid crystals R-41 (temperature range, 41-45 °C) were used as described in Section C.1.c of Chapter II, Description of Experimental Apparatus. The color pattern obtained on the liquid crystals appeared cloudy and "grainy". The author concluded that the extremely transient and random conditions of dropwise condensation and the numerous small drops on the condensing surfaces (See Figures 13 and 14.) occurred too fast and in too small an area to influence the liquid crystals color patterns. In the case of nucleate boiling, Raad and Myers [59] counted the number of nucleation sites on stainless steel during experiments at different heat fluxes. For a heat flux of 77.3 kW/m^2 (24,500 $Btu/hr\text{-}ft^2$), they counted an average of 8820 sites per square meter (820 per square foot). They also found that the number of nucleation sites did not change as a function of time. During dropwise condensation, however, from the work of McCormick and Baer [15] for stainless steel promoted with benzyl mercaptan in the horizontal position, and at sub-atmospheric pressure, the nucleation density was found to be 8.3×10^5 sites per square centimeter.

Rather than pursuing the use of liquid crystals further, it was decided to use only thermocouples to measure the condensing foil temperature.

2. High-speed Motion and Still Pictures

The process of dropwise condensation can be studied very effectively using high-speed motion pictures through a magnifying lens. This author recorded the phenomenon at speeds of 160, 600, and 920 frames per second through a lens which gave a magnification of 20X. The highest speed was most beneficial to study the dropwise condensation process, as it allowed a thorough observation of the growth of a drop until it swept down the surface.

Figures 13 and 14 were taken with a single-lens reflex still camera. Pictures of this type allow the observer to see how many and what size drops are on the surface at an instant in time and to see the difference in drop size caused by condenser surface inclination.

3. Brush Recorder Temperature Traces

The Brush recorder allowed the author to record the temperature of a selected thermocouple for any length of time during a run. Figures 15, 16, and 17 show temperature traces taken for various experimental conditions. Figures 15 and 16 can be compared to show the effect of condenser surface thermal properties, and Figures 16 and 17 can be compared to show the effect of non-condensable gas (i.e., air being driven out of the boiler water) on the surface temperature at the thermocouple located near the top of the condensing surface. These effects on dropwise condensation will be discussed more fully in Section E of this chapter.

C. FILMWISE CONDENSATION RESULTS

Several attempts were made to get complete filmwise condensation on the copper surfaces so that a comparison could be made with the Nusselt [1] theory. The quality of the obtained filmwise condensation was unsatisfactory as the mixed mode of condensation was always present.

The problem was first analyzed as a contamination of the condensing chamber with promoters of dropwise condensation from previous experiments. Attempts at cleaning the condensing chamber with alcohol, acetone, and dilute sulfuric acid provided the same mixed condensation. At this point, a new condensing chamber was manufactured of glass and aluminum. However, even with this new condensing chamber, it was still not possible to achieve complete filmwise condensation on the foil at atmospheric or sub-atmospheric pressures.

It was then decided to use thicker material for the condenser surface. For a short period under sub-atmospheric conditions, filmwise condensation was achieved on the 3.18 mm (0.125 in) thick copper plate. Once atmospheric pressure was reached, however, the condensation changed to the mixed mode and would not return to filmwise.

The author has no explanation for this problem but includes it for completeness.

D. HEAT TRANSFER DATA PRESENTATION AND DISCUSSION

In the paper of Le Fevre and Rose [20], the authors pointed out that the traditional plot of heat transfer

coefficient versus heat flux can be misleading when errors in the temperature difference ($T_{vap} - T_w$) were appreciable. Therefore, in addition to plotting the heat-transfer coefficient versus the heat flux, this author has plotted heat flux versus the temperature difference between the vapor and the condensing surface. Where appropriate, the heat transfer coefficient was plotted against the parameters being changed.

1. Effects of Thermal Properties of the Condenser Surface

One of the objectives of this work was to carry out dropwise condensation using liquid crystals to determine the temperature pattern on the condensing surface. Thin foils of low heat capacity were therefore required as the condenser surface.

In addition, different thermal properties or resistances for the condenser surfaces were achieved by using two types of copper foils, one plain and one covered with Mylar, by using a thicker copper plate, and by using a different condenser material, titanium. The effects of these thermal resistances are shown in Figures 18 and 19 for the calculated results and in Figures 15 and 16 for the temperature fluctuations caused by the different condenser materials.

The effect of condenser surface thickness is shown in Figure 19 by the large reduction of the temperature difference ($T_{vap} - T_w$) as the condenser thickness increases.

This decrease in temperature difference substantially increases the heat transfer coefficient as seen in Figure 18. The reason for the increase in heat transfer coefficient for the thicker condenser surface was proposed by Hurst and Olson [26]. They stated that thinner condenser surfaces were not as capable as thicker surfaces in dissipating heat laterally from the edge of each drop out into the condenser material.

The Mylar on the cooling side of the copper foil greatly reduced the heat flux through the condenser surface, well below the heat flux for the plain copper foil. With the lower heat flux and smaller temperature difference between the vapor and the condensing surface, the chances for error in the reduced data became greater. Although the effect of the addition of Mylar cannot be stated conclusively, it appears to give a slightly higher heat transfer coefficient than the plain foil.

The copper foil shows a higher heat transfer rate than the titanium foil of the same thickness when runs of similar boiling times are compared. It should be noted that the titanium foil was undergoing mixed condensation and the copper foil was undergoing dropwise condensation. Figures 15 and 16 show the surface temperature fluctuations of a copper foil undergoing dropwise condensation and a titanium foil undergoing mixed condensation. The temperature fluctuations on the copper foil are considerably less

than on the titanium foil. A possible reason for the larger fluctuations on the titanium foil could be the mixed condensation occurring on the titanium surface. It also could be due to the lower thermal conductivity of the titanium surface which could be diffusing the heat outward from each drop perimeter slower than the higher conductivity copper surface.

Most of the existing experimental studies [30, 68,69] and one theoretical analysis [29] have shown an increase in the heat transfer coefficient with an increase in condenser thermal conductivity. In one experiment, however, Aksan and Rose [31] observed no significant effect of thermal properties of condensing surface materials on identically copper-plated plates of copper and stainless steel. In all the work except [68], the condenser surfaces were plated or coated in an identical fashion.

2. Effects of Non-Condensable Gas

The effect of non-condensable gases (i.e., air) has been shown conclusively by this and previous works to decrease the heat-transfer coefficient. Figures 20 and 21 show the effect on the coefficient by just the air that is boiled out of the boiler water. After several hours of boiling, the value of the heat transfer coefficient increases. Tanner, Pope, Potter, and West [70] experimented by introducing nitrogen into the inlet steam. They found the magnitude of the reduction in the heat-transfer

coefficient to be dependent upon 1) heat flux, 2) steam pressure, and 3) the concentration of non-condensable gas in the bulk steam.

A comparison of Figures 16 and 17 shows the temperature fluctuations at a specific thermocouple for the same test conditions except for air being given off from the boiler water. The fluctuations of the surface temperature drop from about 25 °C down to less than 10 °C, after nine hours of boiling.

Similar results were obtained by Le Fevre and Rose [35], and they attribute the fluctuations to the presence of non-condensable gas from air being given off by boiling. They further claim that even prolonged boiling will not reduce significantly the amount of non-condensable gas in the water.

The vapor velocity is also an important factor in removing non-condensable gases from the vicinity of the condensing surface. In their work, Welch and Westwater [9] used a vapor velocity past their copper condensing surface of half that of the present work with a resultant lower heat-transfer coefficient than in the present work. They stated that the non-condensable gas content of their system was between 10 and 13 parts per million. Tanner, Potter, Pope, and West [71] and O'Bara, Killian, and Roblee [72] also studied the dependence of the heat transfer coefficient on vapor velocity. They observed a significant increase in the heat transfer coefficient with increased vapor velocity.

3. Transient Effects

Promoters that are brushed or sprayed onto the condensing surface are generally applied in too heavy a coating to enhance properly dropwise condensation. The extra promoter material acts as a thermal resistance to heat transfer and usually results in a decrease in the heat transfer coefficient. It has been shown [25,56,73] that the heat transfer coefficient rises with time after condensation begins and subsequently reaches a steady-state value, all other factors remaining constant. Figure 22 shows agreement with the previous workers. One difference between the work of Graham [25] and Moreno [56] and that of Citakoglu and Rose [73] and the present work is the lack of a peak prior to reaching steady state in the last two works. Graham [25] attributes the differences in the transient curves to different surface-promoter characteristics.

4. Effect of Condensation Mode

Figures 23 and 24 show the effect of the different modes of condensation, all on the same condenser surface. As would be expected, filmwise condensation produces the greatest vapor-to-surface temperature difference and the smallest heat transfer coefficient. As the condensing plate progressively became more dropwise, the temperature difference decreased and the heat transfer coefficient increased toward that obtained for dropwise condensation.

A recently proposed theory by Takeyama and Shimizu [74] suggests that there exists a condensing curve similar to the well-known boiling curve. Figure 25 is a reproduction of the proposed condensing curve. The authors describe the condensation process as follows. (Refer to Figure 25.) Dropwise condensation occurs at low vapor-to-surface temperature differences. The dropwise process continues until a vapor-to-surface temperature difference of about 80 °C is reached. At this point the transition regime begins where dropwise condensation changes to filmwise condensation. This transition condensation is compared to transition boiling on the boiling curve. Decreasing the vapor-to-surface temperature difference does not cause the process to go back into the dropwise condensation region, but rather the change progresses along the filmwise curve toward the origin. At a transition point on the filmwise curve, the water film breaks and droplets form, bringing the state suddenly to a point in the dropwise region.

As seen from Figure 25, Takeyama and Shimizu [74] presented data which in the case of dropwise condensation was considerably higher than the other investigators [21,33,69], and the filmwise condensation data was much higher than the calculated data from the Nusselt theory. A possible reason for the disparity of the data is the comparative sizes of the different condensing surfaces. The authors [74] used an extremely small condensing

surface area (25 sq mm) with a greatly enlarged cooling surface area (3600 sq mm). The smallest condensing area of the other authors was that used by Tanner, Pope, Potter, and West [69], who used a condensing surface area of 285 sq mm.

The data of the present work can also be seen to be much lower than that of Takeyama and Shimizu [74], the present dropwise condensation data being even lower than their filmwise condensation data. Possible reasons for the lower data of the present work could be the difference in the condenser surface area, as mentioned above, or the non-condensable gas content in the present work which greatly reduced the heat transfer coefficient. The authors [74] showed a considerable decrease in heat flux for steam with air (0.0045 kg air/kg steam), as shown by the dotted line on Figure 25. Another possible reason for the lower data for the present work is the effect of the thinner condenser surfaces. The minimum thickness used for any of the mentioned authors was 38 mm compared to a maximum thickness of the present work of 3.18 mm. The thicker condenser surfaces may have different transient conduction behavior than the thinner condenser surfaces. The difference in heat flux values is even more noticeable for the thinner, 0.051 mm thick, copper foils.

Notwithstanding the lower heat flux values when compared to the other authors [21,33,69,74], the data of the present work could similarly form another condensing

curve, as shown on Figure 25. This would indicate that there could be a different condensing curve for each set of condensation conditions, such as condenser surfaces, pressures, surface finish, etc.

5. Surface Inclination Effects

Figure 26 compares results from the present work to that of other investigators for the effect of surface inclination on dropwise condensation. Agreement in general is quite good over the range of values compared with other investigators [33,34,53,75]. One may note in Figure 26 that the curve for Citakoglu and Rose [33] has a second maximum around 120 degrees. Citakoglu and Rose claim this is due to a small change in the vapor-to-surface temperature difference with variation in inclination, measured by them but not by others. As can be seen from Figure 26, the heat transfer coefficient is reasonably constant 60 degrees from the vertical position, where the coefficient is largest. It would stand to reason that the vertical position would cause early departure of drops and rapid sliding speeds, thus giving the best heat transfer [25].

However, as is shown in Figure 26, even at the horizontal position, the heat transfer coefficient is reduced only by about 50 percent of the maximum value at the vertical position. This is especially surprising when Figures 13 and 14 are compared. Figure 14 shows the drops on the horizontally oriented condensing surface to

be many times the size of the drops on the vertical surface, Figure 13. Thus the number of inactive drops on the horizontal surface should cause a decrease in the heat transfer coefficient. Citakoglu and Rose [33] used this observation to conclude that the average heat transfer for the whole plate is only weakly dependent on maximum drop size.

V. CONCLUSIONS AND RECOMMENDATIONS

A. CONCLUSIONS

1. Any non-condensable gas concentration, however small, reduces the heat transfer coefficient significantly during dropwise condensation. Non-condensable gases also cause large surface temperature fluctuations, resulting in difficulties of accurately measuring heat transfer coefficients.

2. Angles of inclination greater than 60 degrees past the vertical position significantly reduce the heat transfer coefficient during dropwise condensation.

3. For thin foils, the value of the heat transfer coefficient is significantly affected by changing the condenser surface from copper to titanium.

4. For a copper surface, the heat transfer coefficient increases by a factor of five when the condenser surface thickness increases from 0.051 mm (0.002 in) to 3.18 mm (0.125 in).

5. Chemical promoters that are brushed onto the condensing surface are applied too thick to promote good dropwise condensation and require a period of time, depending on promoter and surface material used, to "wash" off. The value of the heat transfer coefficient rises sharply immediately after condensation begins on a newly promoted surface until it reaches a steady value. The

time required for the heat transfer coefficient to reach its steady value is about two hours after condensation begins on the surface.

6. Promoters which promote dropwise condensation well on copper surfaces do not promote good dropwise condensation on titanium surfaces. Both n-octadecyl mercaptan and oleic acid, which have high affinity for copper, "wash" off titanium surfaces, resulting in mixed mode condensation.

B. RECOMMENDATIONS FOR FURTHER WORK

1. Fix the mass flow rate of cooling water to avoid changes in the flow regime and control the heat flux by controlling the cooling water inlet temperature.

2. Increase the power to the boiler to allow for greater steam velocity past the condensing surface.

3. Design a closed-loop system to allow for longer run times and eliminate stopping during a run to refill the boiler with water.

4. Further investigate the effects of test surface thickness on dropwise condensation to determine, in fact, if there is a minimum condenser wall thickness to be used with dropwise condensation.

5. Investigate promoters which have a high affinity for titanium and stainless steel to determine their effectiveness on dropwise condensation.

6. Investigate polymer coatings for use as dropwise condensation promoters.

7. Investigate filmwise condensation on thin foil condenser materials in view of problems encountered in this work. Determine if there is a lower temperature difference limit between the vapor and the condensing surface in order for filmwise condensation to occur.

8. Further investigate dropwise condensation with the high-speed motion camera to analyze the dropwise condensation phenomenon.

APPENDIX A: THERMOCOUPLE APPLICATION PROCEDURES

1. For the Titanium Surface

Once the thermocouple had been made and the thermocouple bead flattened, the thermocouple was attached to the titanium surface by tack-welding.

A brass support "ring" was then epoxied over the outer edges of the surface over the thermocouple leads to prevent accidental breakage of the thermocouple wires.

2. For the Copper Foils

At first, tack-welding was attempted on the copper foil but was later abandoned. The copper surface conducted the heat away so fast that adjusting the tack-welder to the correct amperage was extremely difficult. Either the amperage was too low to fuse the thermocouple bead to the surface or it was too high and would arc on the surface between the electrodes. The arc from the electrode always left a hole in the foil.

Therefore, soldering was used. The procedure utilized two hot plates, one at about 315 °C and the other at about 150 °C. The copper surface was placed on the hotter plate and allowed to come up to that temperature. At this point solder was touched to the surface where the thermocouples were to be attached, leaving a mound of molten solder. The surface was then placed on the second

hot plate. This hot plate brought the solder almost up to the melting temperature. The thermocouple bead was positioned on the mound of solder. The solder was melted with a soldering iron while the bead was positioned with a probe. When the soldering iron was removed, the solder solidified and held the thermocouple bead in place. The brass "ring" was added to the copper foil to prevent breakage of the beads.

3. For the Copper Plate

The procedure for the copper plate was essentially the same as the soldering procedure for the copper foil, with two exceptions. First, the thermocouple leads were epoxied into the grooves machined in the copper plate. Second, no brass support was needed over the thermocouple leads since they were supported by the epoxy glue holding them into the groove.

APPENDIX B: CALIBRATION OF INSTRUMENTS

1. Thermocouples

Temperature measurement plays a very important part in heat transfer calculations. The accuracy of this measurement becomes even more critical during dropwise condensation due to the small temperature differences experienced between the vapor and condensing surface.

To achieve the desired accuracy, all thermocouples were calibrated at one time using a Rosemount Engineering Company Model 913A Variable Temperature Oil Bath for a temperature range of 20 to 105 °C. The thermocouples were suspended in the oil bath with their leads connected to a Newport Digital Pyrometer.

A Platinum Resistance Thermometer connected to a high precision Commutating Bridge Model 920A was used as the standard for the bath temperature. This system provided an accuracy of ± 0.002 °C.

The nominal temperature was set for the bath, and the bath was allowed to settle for five minutes for each temperature point. The thermocouples were read on the Newport Digital Pyrometer directly in degrees C. The value of the Platinum thermometer was read from the bridge in ohms and converted to degrees C from conversion tables provided by the manufacturer of the thermometer.

The value for each thermocouple was compared to the value of the Platinum thermometer for the set temperature. Readings were taken at 5 °C intervals, and the corrections were assumed linear between data points.

Table 1 shows the correction to be applied to each of the thermocouple groups used in the heat-transfer measurements.

2. Quartz Crystal Thermometers

The quartz crystal thermometers were calibrated using the same calibration procedures as for the thermocouples in Section 1 of this appendix. Since it is essential to know the temperature differences of the cooling water as accurately as possible, smaller intervals, 2 °C were used in calibrating the quartz thermometers. The thermometers were calibrated between 10 and 35 °C.

The difference between each quartz crystal thermometer and the Platinum standard was taken and put into tabular form for use as corrections to the readings. This list of corrections is found in Table 2.

3. Flowmeter

To control the circulation of tap water over the cooling side of the condensing surface, a constant cross section Precision Bore Flowrator Tube FP-1/2-27-G-10/83 with a maximum flow of 1.12 gallons per minute (4.23 kilograms per minute) was used. The amount of cooling

water flowing over the condensing surface has a substantial influence on the heat-transfer measurement; thus calibration was necessary to eliminate a source of error.

The flowmeter was calibrated over the entire range of the scale in increments of 10 percent. To measure the amount of water through the flowmeter, a Toledo Scale with a capacity from 0-40 pounds and marked in increments of 0.1 pound was used. An electric timer measuring 0.1 second was used to time the flow into a container resting on the scale.

The net difference in weight was divided by the time to give the mass flow rate of water.

Table 4 gives a summary of the calibration of the flowmeter.

APPENDIX C: PROCEDURES FOR USING AND INTERPRETING THE BRUSH RECORDER

During dropwise condensation, the temperatures of the different thermocouples were observed to fluctuate. It was decided to record this fluctuation for several different experimental conditions. To provide data that could be compared, thermocouple number 6 was selected as the one to be recorded. This thermocouple is located nearest the top of the surface as shown on Figure 12.

The thermocouple leads were disconnected from the Digital Pyrometer and connected to the preamplifier of the Brush Recorder. The sensitivity of the recorder was set to 20 microvolts per division, and the zero suppression control was used to position the pen trace on the chart paper. The recorder was run at 5 mm per second and 50 mm per second to record the temperature for at least one minute.

The thermocouple leads were then disconnected; and without touching any control knobs, a Leeds and Northrup student potentiometer was connected to the preamplifier junction. The potentiometer had been zeroed and standardized previously according to the manufacturer's instructions. The potentiometer voltage was then adjusted, with the recorder running at 5 mm per second, to mark several positions on the chart. The value in millivolts at each

of these positions was recorded. The temperature at the thermocouple junction was taken with a precision thermometer, and the converted value in millivolts was added to each of the values marked above. The sums of the two millivolt readings at each position were converted to temperature in degrees C using standard Copper-Constantan thermocouple conversion charts.

APPENDIX D: UNCERTAINTY ANALYSIS

The uncertainties for the calculations of this work were estimated by the method proposed by Kline and McClintock [76] for Single-Sample experiments. The relationships used to determine the final results are as follows:

$$q/A = \frac{\dot{m}_{cw} C_p \Delta TQ}{A} \tag{D-1}$$

$$\Delta T_w = \frac{q/A \ \Delta X_w}{k_w} \tag{D-2}$$

$$\bar{h}_{ss} = \frac{q/A}{(T_{vap} - T_w)} \tag{D-3}$$

Theorem 3 of Kline and McClintock gives this relationship for $\underline{n}$ independent variables and the result

$$w_R = [(\frac{\partial R}{\partial v_1} w_1)^2 + (\frac{\partial R}{\partial v_2} w_2)^2 + \ldots + (\frac{\partial R}{\partial v_n} w_n)^2]^{1/2} \tag{D-4}$$

when the result, R, is a linear function of the $\underline{n}$ independent variables $v_1,\ldots,v_n$ and where w_R is the interval for the result and w_i is the interval for the ith variable. An additional step taken to simplify Equation (D-4), is to divide through by the result to

nondimensionalize the terms and give the uncertainty in a percentage form. Equation (D-4) then becomes

$$\frac{w_R}{R} = \left[\left(\frac{1}{R}\frac{\partial R}{\partial v_1} w_1\right)^2 + \left(\frac{1}{R}\frac{\partial R}{\partial v_2} w_2\right)^2 + \ldots + \left(\frac{1}{R}\frac{\partial R}{\partial v_n} w_n\right)^2\right]^{1/2} \tag{D-5}$$

Putting Equations (D-1) - (D-3) in the form of Equation (D-5) gives

$$\frac{w_{q/A}}{q/A} = \left[\left(\frac{w_{\dot{m}}}{\dot{m}}\right)^2 + \left(\frac{w_{c_p}}{c_p}\right)^2 + \left(\frac{w_{\Delta TQ}}{\Delta TQ}\right)^2 + \left(-\frac{w_A}{A}\right)^2\right]^{1/2} \tag{D-6}$$

$$\frac{w_{\Delta T_w}}{\Delta T_w} = \left[\left(\frac{w_{q/A}}{q/A}\right)^2 + \left(\frac{w_{\Delta X_w}}{\Delta X_w}\right)^2 + \left(-\frac{w_{k_w}}{k_w}\right)^2\right]^{1/2} \tag{D-7}$$

$$\frac{w_{\bar{h}_{ss}}}{\bar{h}_{ss}} = \left[\left(\frac{w_{q/A}}{q/A}\right)^2 + \left(-\frac{w_{(T_{vap} - T_w)}}{(T_{vap} - T_w)}\right)^2\right]^{1/2} \tag{D-8}$$

Using the above three equations, the uncertainties for four runs were calculated. The results of these calculations are shown in Table 5.

The uncertainties for each of the variables must be known before Equations (D-6) - (D-8) can be used for the result.

The mass flow rate of the cooling water, $\dot{m}_{cw}$, has uncertainties associated with its calibration and

uncertainties in the flow which might be caused by fluctuations in the water supply. The calibration of the flowmeter is discussed in Appendix B. The calibration is outlined briefly below:

$$\dot{m}_{cw} = \frac{W}{t}\frac{g_c}{g} = \frac{m}{t} \quad \text{(since } g = g_c \text{ at sea level)}$$

where

W is in lbf,

m is in lbm, and

t is in seconds.

$w_m = 0.1$ lbm,

$w_t = 0.1$ sec.

$$\frac{\dot{w}_{m_w}}{\dot{m}_w} = \left[\left(\frac{0.1}{m}\right)^2 + \left(-\frac{0.1}{t}\right)^2\right]^{1/2} \qquad \text{(D-9)}$$

The maximum fluctuations of the flowmeter during operation was observed to be ± 2 percent while operating at 60 percent of maximum flow. This gives a worst case uncertainty for the fluctuation of the flowmeter of $0.048\ \dot{m}_{cw}$. Therefore, the total uncertainty of the flowmeter is

$$\frac{\dot{w}_{m_w}}{\dot{m}_{cw}} + 0.048\ \dot{m}_{cw}.$$

The uncertainty of the specific heat, C_p, is taken to be 0.001 kJ/kg - °C.

The uncertainty of the area, A, is 0.070 due to the glue on the foil support covering part of the cooling surface.

The uncertainty of the cooling water temperature difference is found by using the relationship

$$\frac{{}^{w}\Delta TQ}{\Delta TQ} = \left(\frac{0.03}{\Delta TQ}\right)$$

since each quartz crystal thermometer has an uncertainty of 0.02 °C.

Equation (D-2) is used only when either the titanium foil or the copper plate is the condensing surface to extrapolate to get the steam-side wall temperature. The steam-side wall temperature for the copper foil is taken as the temperature read from the thermocouples. This is so because of the small thickness and high conductivity of copper.

The conducting wall thickness, ΔX_w, has an uncertainty associated with it of 0.0254 mm since the thickness was read with a micrometer calibrated to 0.001 in.

The uncertainty for the thermal conductivity, k_w, can be assumed to be ± 5 percent of given values.

Uncertainty for the vapor thermocouples can be contributed from calibration, conduction through the leads,

radiation from the heated observation port and uncertainty of the Digital Pyrometer output. Uncertainties are estimated to be:

Calibration	0.02 °C
Conduction through leads	0.05 °C
Radiation	0.05 °C
Digital Pyrometer	0.20 °C
Total:	0.32 °C

The uncertainty for the test surface results from the above plus an uncertainty for location of the thermocouple to the surface and fluctuations due to the transient nature of dropwise condensation. The author calculated the uncertainty due to the location of the thermocouple bead in the solder to be 0.21 °C using the Hilpert relationship assuming flow of the cooling water over a cylinder (the bead and solder combination). An uncertainty of 1.9 °C was calculated for the fluctuation of temperatures since the fluctuations were usually 3-4 °C.

Thus a total uncertainty for the surface temperature of 2.4 °C is obtained for the thin copper foil.

The copper plate and the titanium foil do not have the uncertainty of the location of the thermocouple bead in that the titanium foil has thermocouples tack-welded

to its surface, and the copper plate has its thermocouples located in a machined slot.

The calculated uncertainties shown in Table 5 are plotted on Figures 18 and 19 to show typical error limits on the calculated heat transfer coefficients and heat fluxes.

TABLE I. THERMOCOUPLE CORRECTION VALUES

Nominal Temperature	0.051 mm Titanium	0.051 mm Copper Plain	0.051 mm Copper w/Mylar	3.18 mm Copper	Steam Vapor
20	-0.9	-1.0	---	-0.4	-0.5
25	-0.9	-1.0	---	-0.4	-0.6
30	-0.9	-1.1	---	-0.4	-0.5
35	-0.8	-1.0	-1.0	-0.4	-0.5
40	-0.8	-0.9	-1.0	-0.4	-0.4
45	-0.7	-0.9	-1.0	-0.4	-0.3
50	-0.8	-0.9	-0.9	-0.3	-0.2
55	-0.7	-0.8	-0.8	-0.4	-0.3
60	-0.6	-0.8	-0.8	-0.3	-0.2
65	-0.6	-0.7	-0.8	-0.2	-0.1
70	-0.5	-0.7	-0.8	-0.2	0
75	-0.4	-0.6	-0.7	-0.2	0.1
80	-0.3	-0.5	-0.6	-0.1	0.2
85	-0.4	-0.5	-0.6	-0.1	0.3
90	-0.5	-0.5	-0.6	-0.1	0.3
95	-0.4	-0.4	-0.6	-0.1	0.3
100	-0.4	-0.3	-0.5	-0.1	0.5
105	-0.3	-0.3	-0.5	-0.1	0.5

TABLE II. QUARTZ CRYSTAL THERMOMETER CORRECTION VALUES

Nominal Temperature	Quartz Crystal Thermometer 1	Quartz Crystal Thermometer 2
10	-0.30	0.12
12	-0.27	0.10
14	-0.28	0.10
16	-0.29	0.09
18	-0.28	0.10
20	-0.30	0.10
22	-0.27	0.11
24	-0.28	0.11
26	-0.27	0.12
28	-0.26	0.12
30	-0.27	0.12
32	-0.25	0.13
35	-0.24	0.14

TABLE III. SUMMARY OF DATA RUNS

Run	Material	Thickness	Condition	Promoter	Condensation Mode
1	Copper	0.051 mm	Foil w/Mylar	Cleaned for filmwise condensation	Attempted filmwise
2	Copper	0.051 mm	Foil w/Mylar	n-octadecyl mercaptan	Dropwise
3	Copper	0.051 mm	Plain foil, cleaned w/ emery paper	n-octadecyl mercaptan	Dropwise
4	Titanium	0.051 mm	As received	n-octadecyl mercaptan	Mixed
5	Titanium	0.051 mm	As received	oleic acid	Mixed
6	Copper	0.051 mm	Plain foil	n-octadecyl mercaptan	Dropwise
7	Copper	3.18 mm	Near mirror finish	Cleaned for filmwise condensation	Filmwise
8	Copper	3.18 mm	Near mirror finish	n-octadecyl mercaptan	Dropwise
9	Copper	0.051 mm	Liquid Crystals attempt	n-octadecyl mercaptan	Dropwise
10	Copper	0.127 mm	Liquid Crystals attempt	n-octadecyl mercaptan	Dropwise

TABLE IV. FLOWMETER CALIBRATION SUMMARY

Percent of Maximum Flow	Mass Flow Rate (kg/sec)	Mass Flow Rate (lbm/sec)
10	0.006	0.012
20	0.013	0.028
30	0.020	0.044
40	0.027	0.060
50	0.034	0.074
60	0.041	0.090
70	0.049	0.109
80	0.055	0.122
90	0.063	0.139
100	0.069	0.152

AD-A040 205 NAVAL POSTGRADUATE SCHOOL MONTEREY CALIF F/G 20/13
SOME EXPERIMENTAL OBSERVATIONS OF DROPWISE CONDENSATION OF STEA--ETC(U)
MAR 77 J L MORGAN

UNCLASSIFIED NL

2 OF 2
ADA
040205

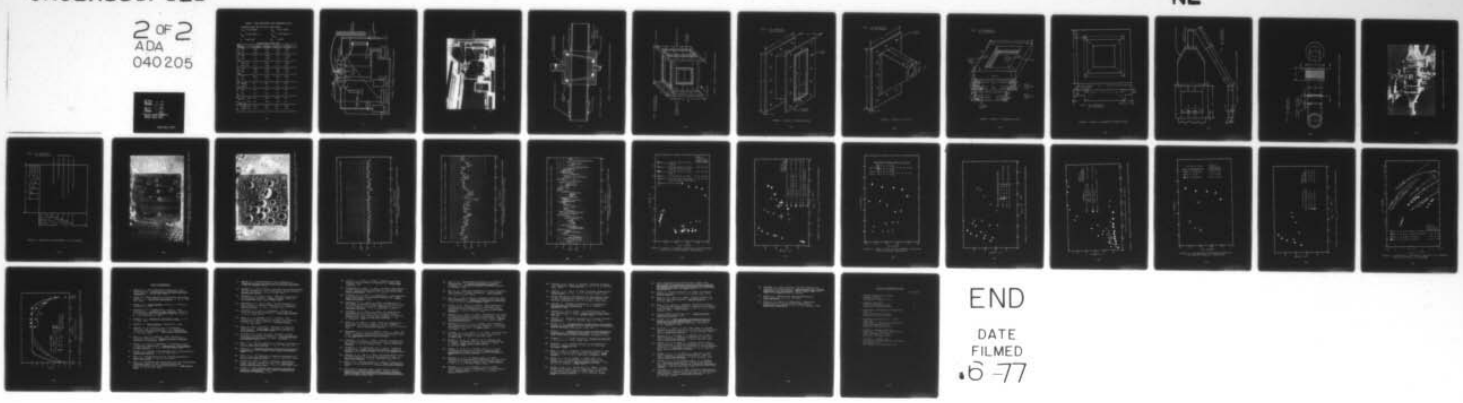

END

DATE
FILMED
6-77

TABLE V. DATA CALCULATIONS WITH UNCERTAINTY LIMITS

Constant values used for runs in this table:

$\dot{m}_{cw}$ = 0.027 kg/sec $\quad w_{\dot{m}_{cw}}$ = 0.001 kg/sec

$c_{p_{cw}}$ = 4.179 kJ/kg - °C $\quad w_{c_{p_{cw}}}$ = 0.001 kJ/kg - °C

A = 645.2 mm^2 $\quad w_A$ = 45 mm^2

Values used for each run:

Run		2	4	6	8
Surface		Cu w/Mylar	Titanium	Plain Cu	Cu Plate
ΔTQ	(°C)	0.43	2.37	2.14	2.65
$w_{\Delta TQ}$	(°C)	0.03	0.03	0.03	0.03
Δx_w	(mm)	----	0.051	----	2.794
$w_{\Delta x_w}$	(mm)	----	0.003	----	0.003
k	(W/m - °C)	----	12.2	----	382.0
w_k	(W/m - °C)	----	0.61	----	19.1
T_{vap}	(°C)	100.0	99.8	99.9	99.9
$w_{T_{vap}}$	(°C)	0.32	0.32	0.32	0.32
T_w	(°C)	96.4	61.5	60.2	87.4
w_{T_w}	(°C)	1.2	2.2	2.4	1.0
q/A	(kW/m^2)	75	415	374	464
$w_{q/A}$	(kW/m^2)	8	33	30	37
T_w	(°C)	----	1.7	----	3.4
w_{T_w}	(°C)	----	0.2	----	0.3
$(T_{vap} - T_w)$	(°C)	3.6	36.6	39.7	9.1
$w_{(T_{vap} - T_w)}$	(°C)	1.2	2.2	2.4	1.0
$\bar{h}$	(hW/m^2 - °C)	20.9	11.3	9.4	50.9
$w_{\bar{h}}$	(kW/m^2 - °C)	7.3	1.1	0.9	6.9

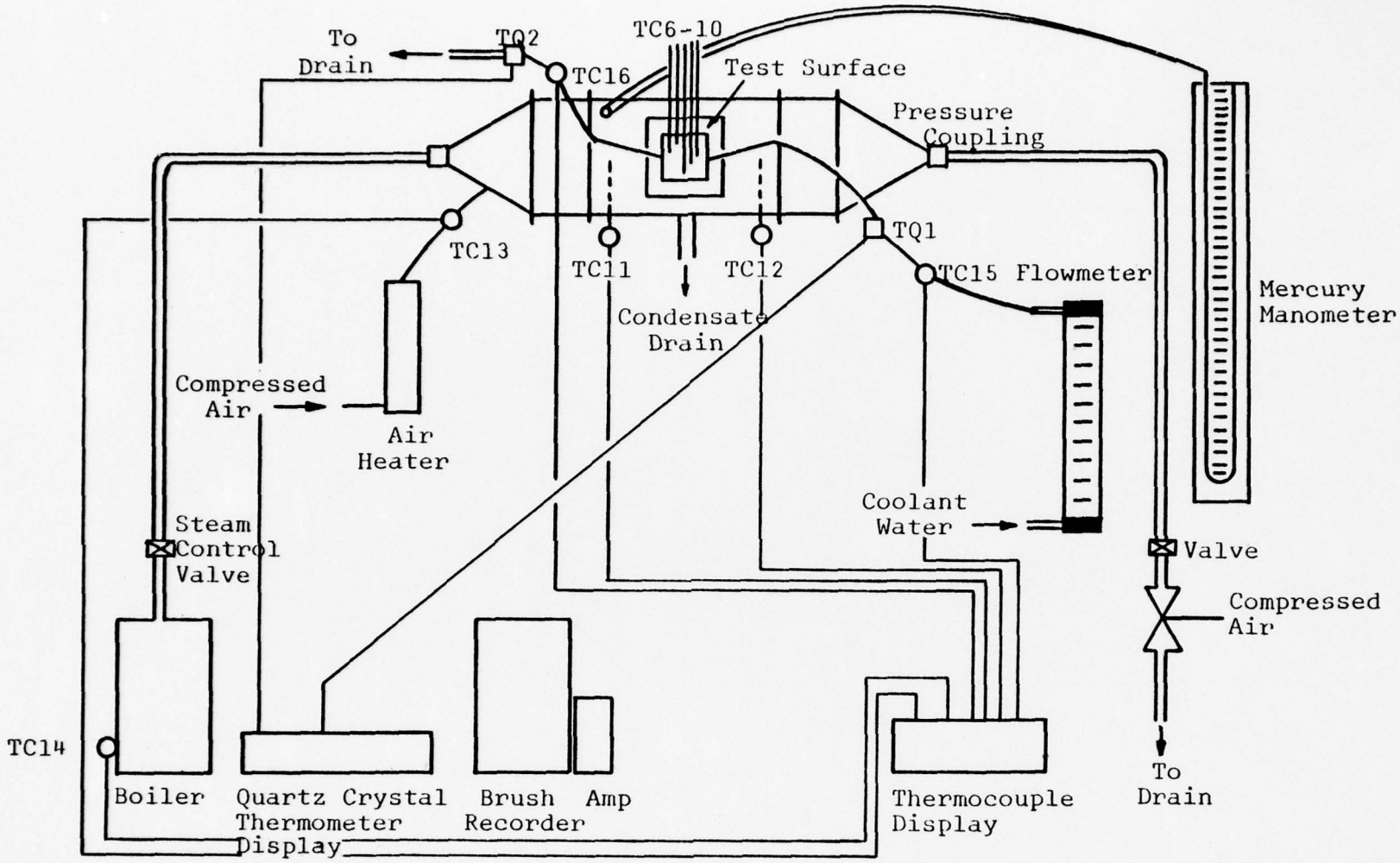

FIGURE 1 SCHEMATIC OF EXPERIMENTAL APPARATUS

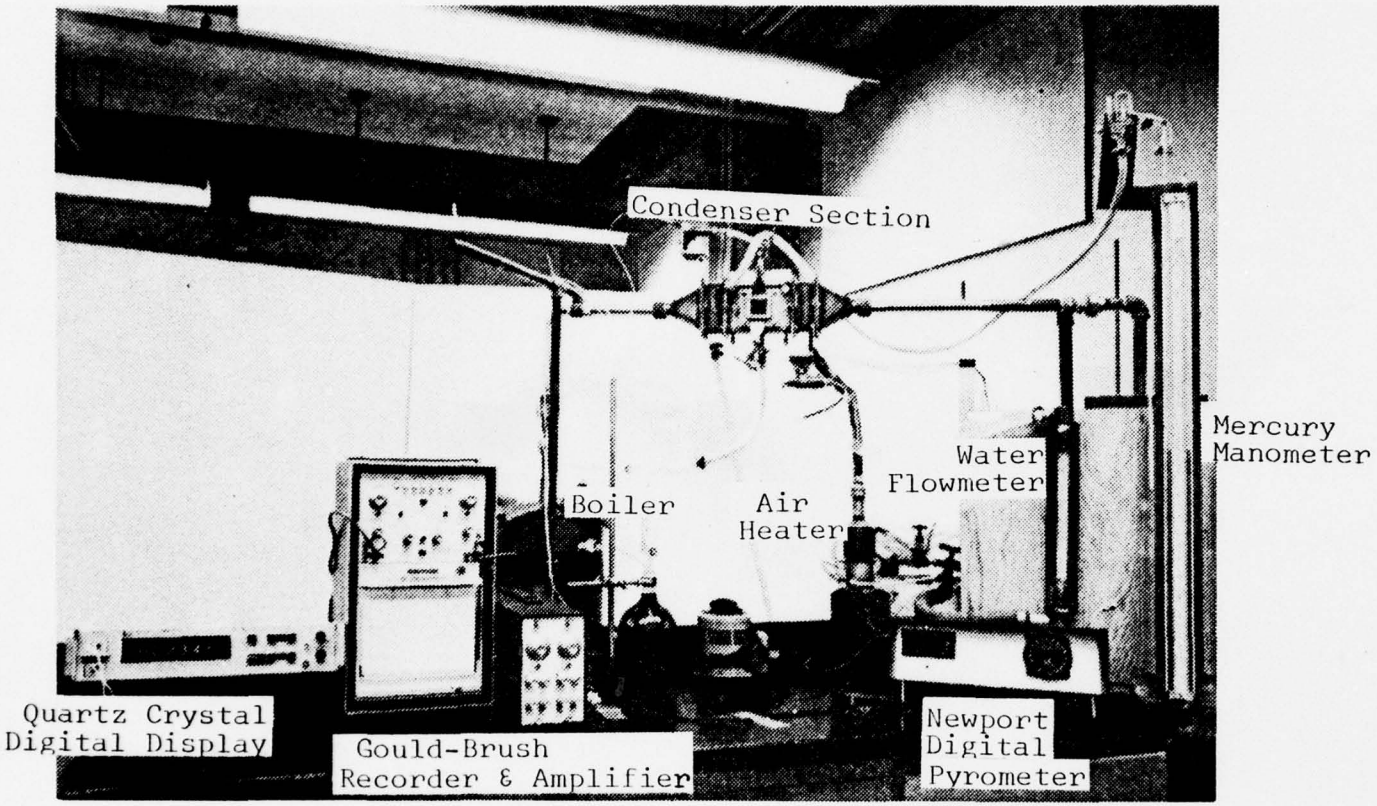

FIGURE 2 PHOTOGRAPHIC VIEW OF EXPERIMENTAL APPARATUS

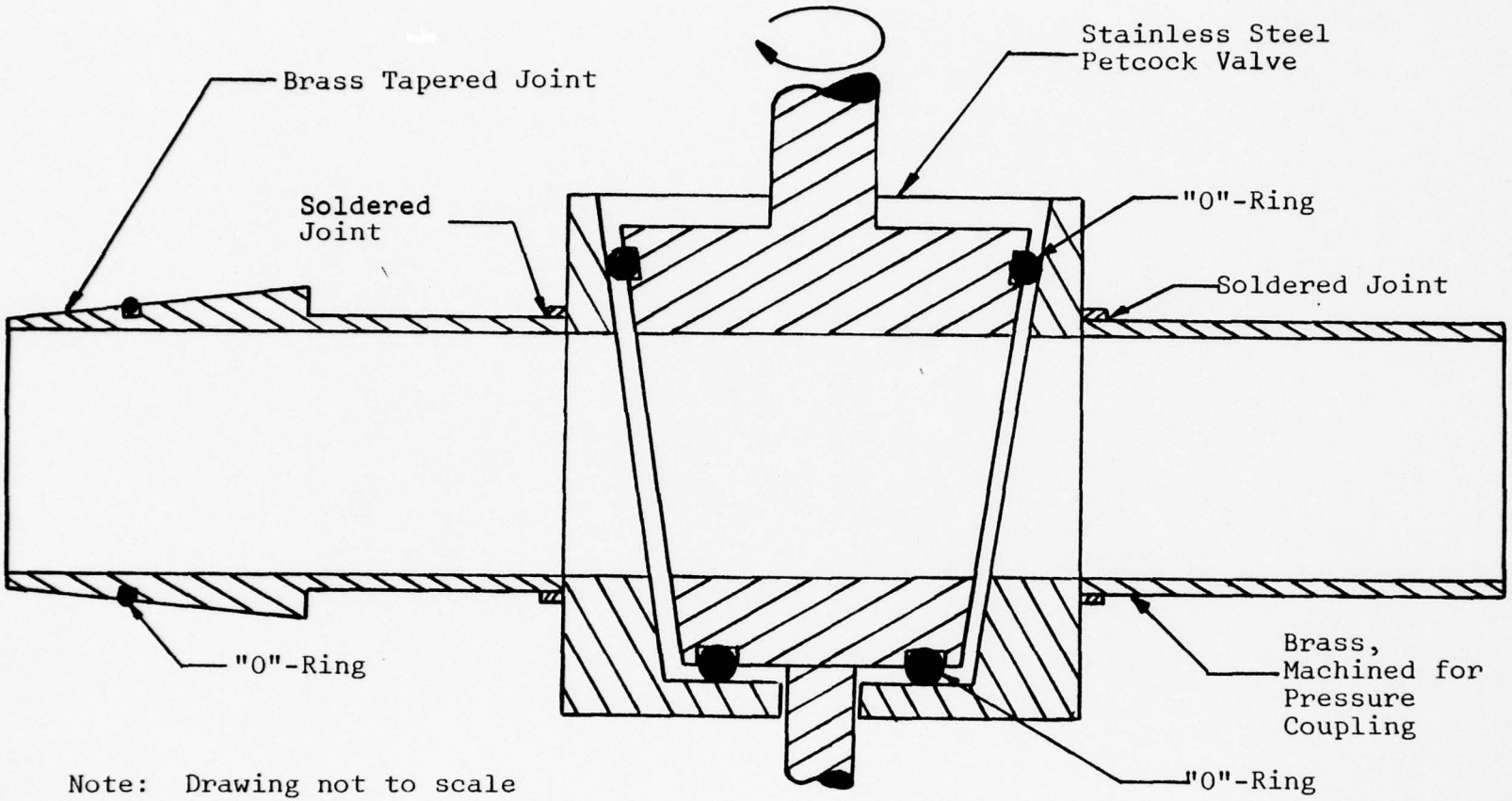

FIGURE 3 DETAILS OF BOILER JOINT/STEAM PETCOCK VALVE

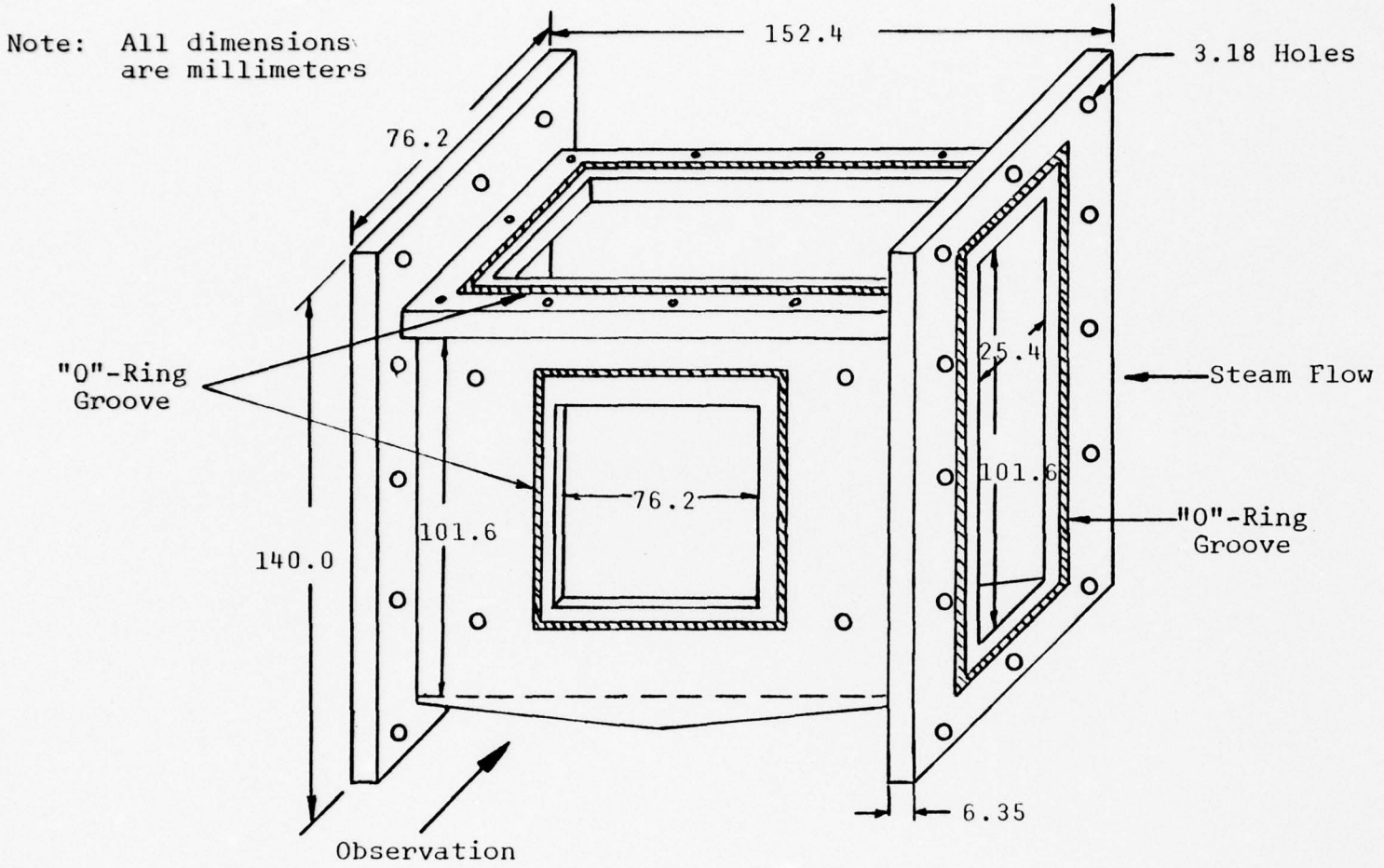

FIGURE 4 DETAILS OF CONDENSING CHAMBER

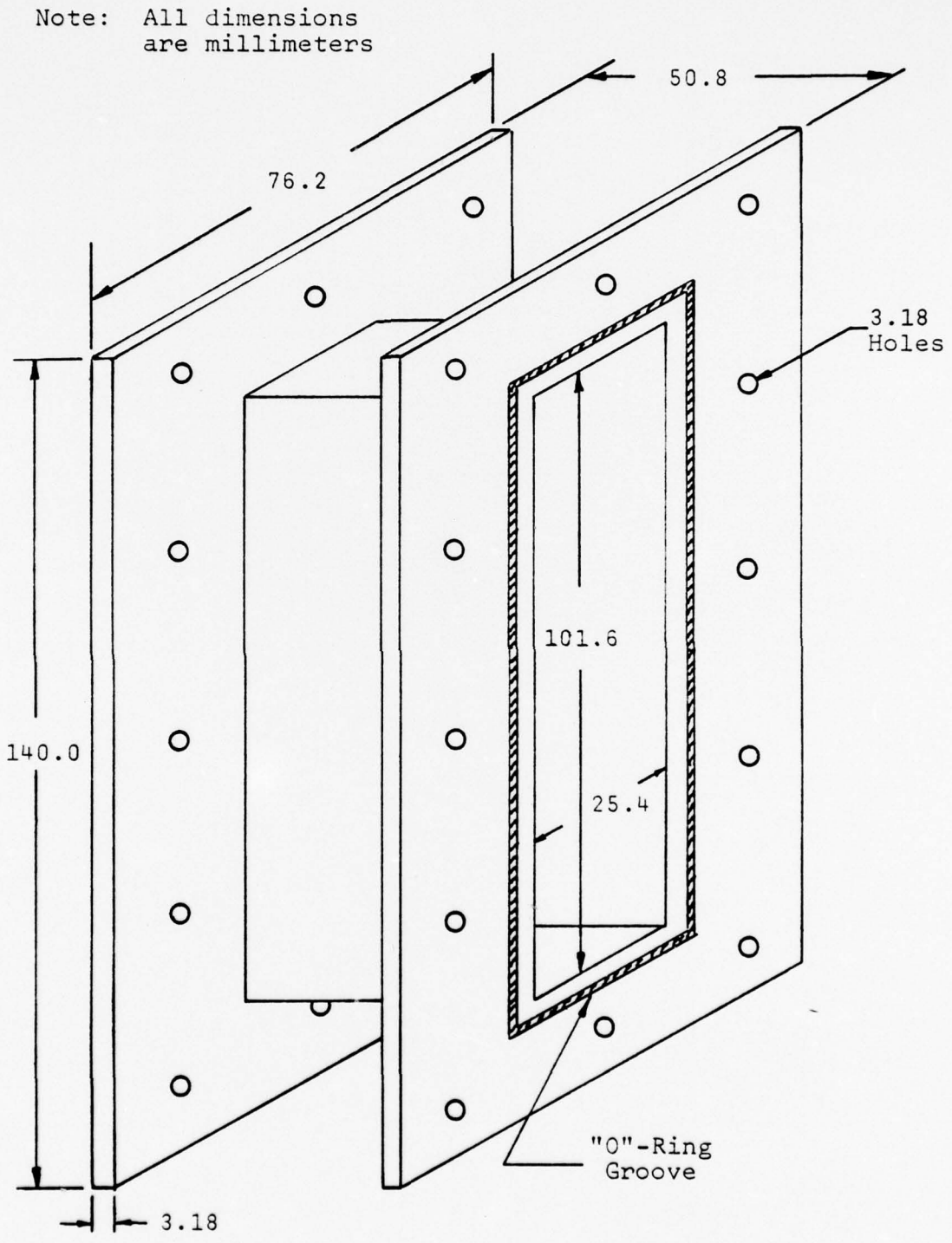

FIGURE 5 DETAILS OF BAFFLE HOUSING

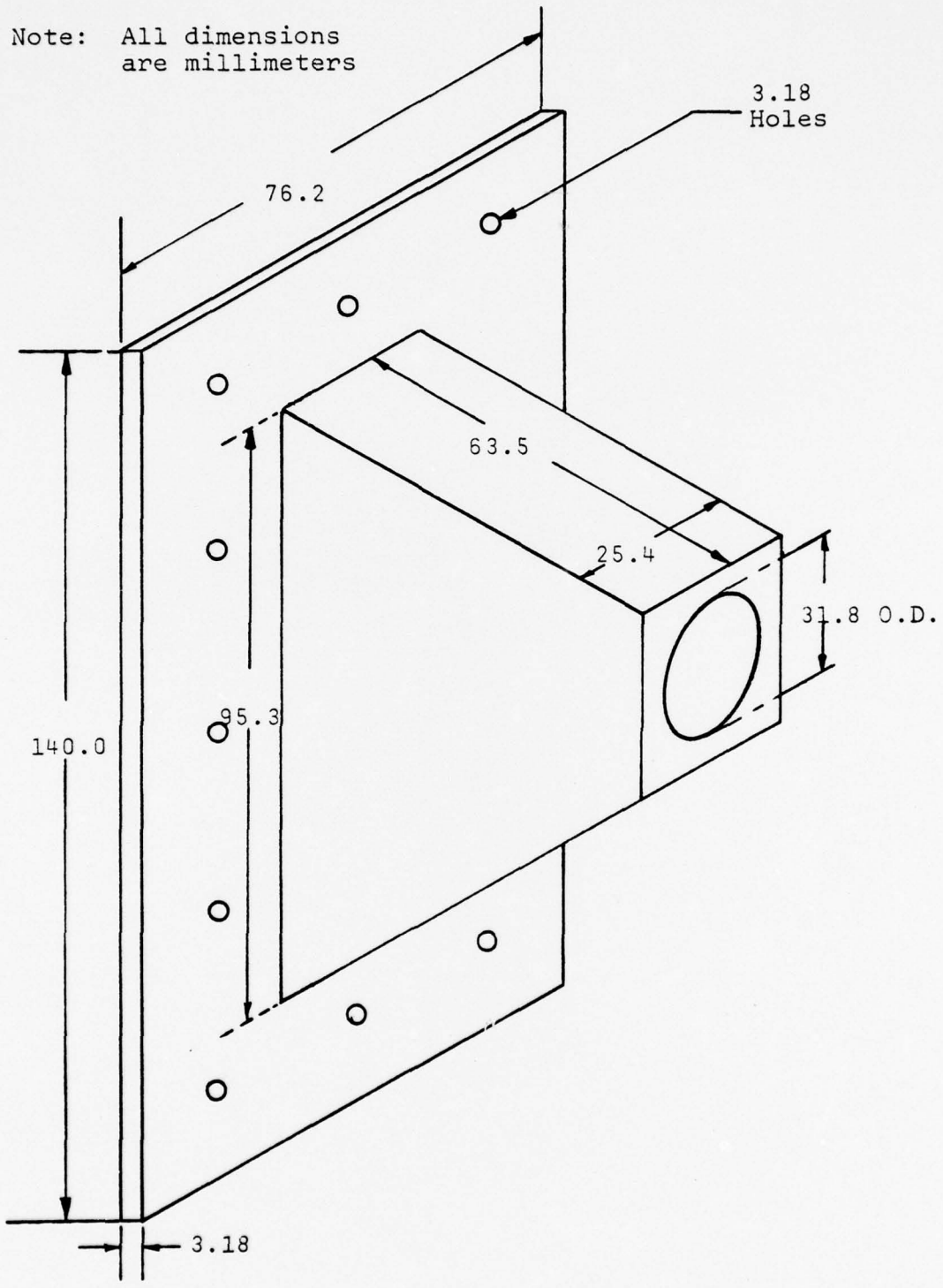

FIGURE 6 DETAILS OF END CAP

Note: All dimensions
are millimeters

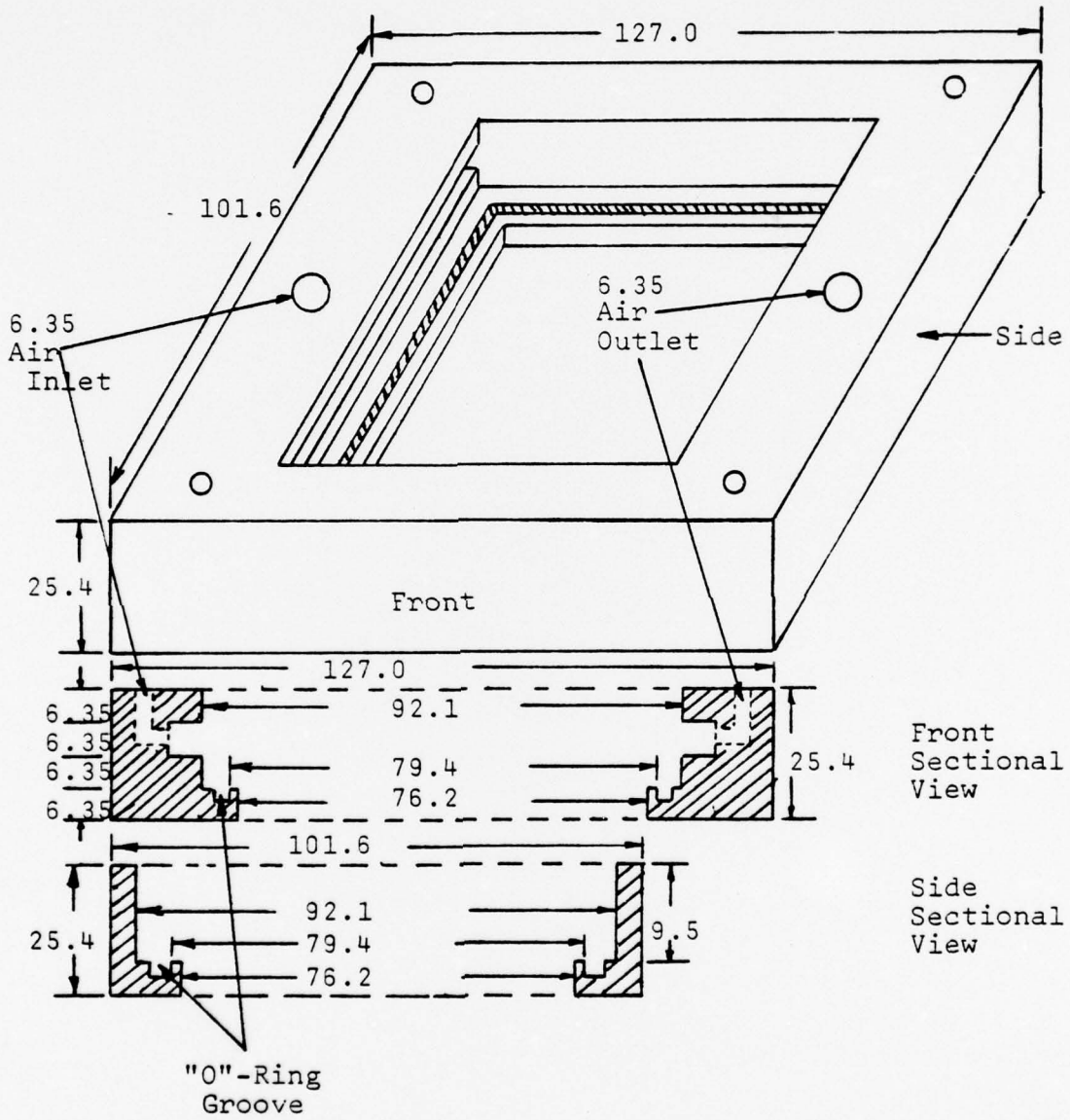

FIGURE 7 DETAILS OF OBSERVATION PORT

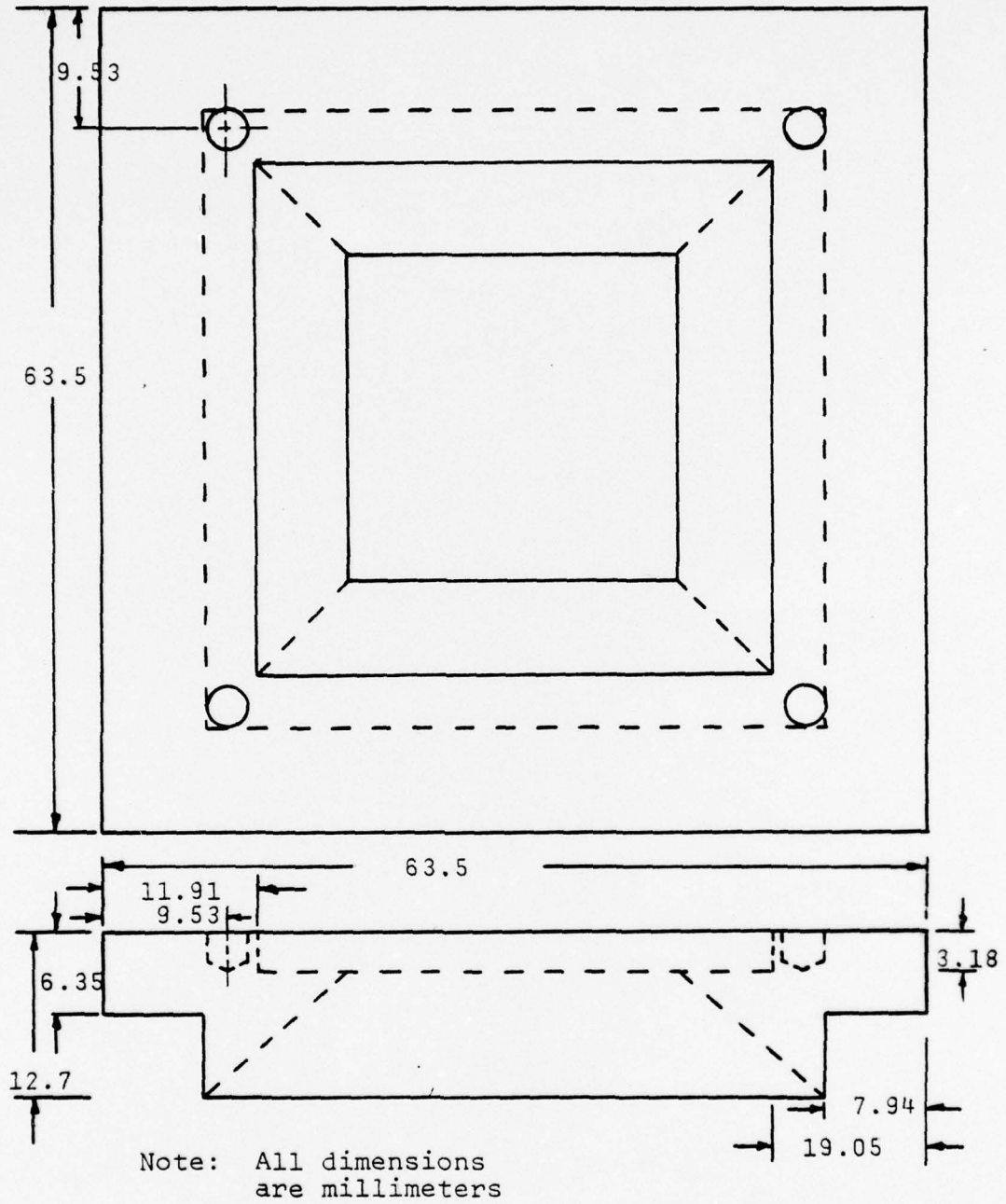

Note: All dimensions are millimeters

FIGURE 8 DETAILS OF CONDENSING CHAMBER INSERT

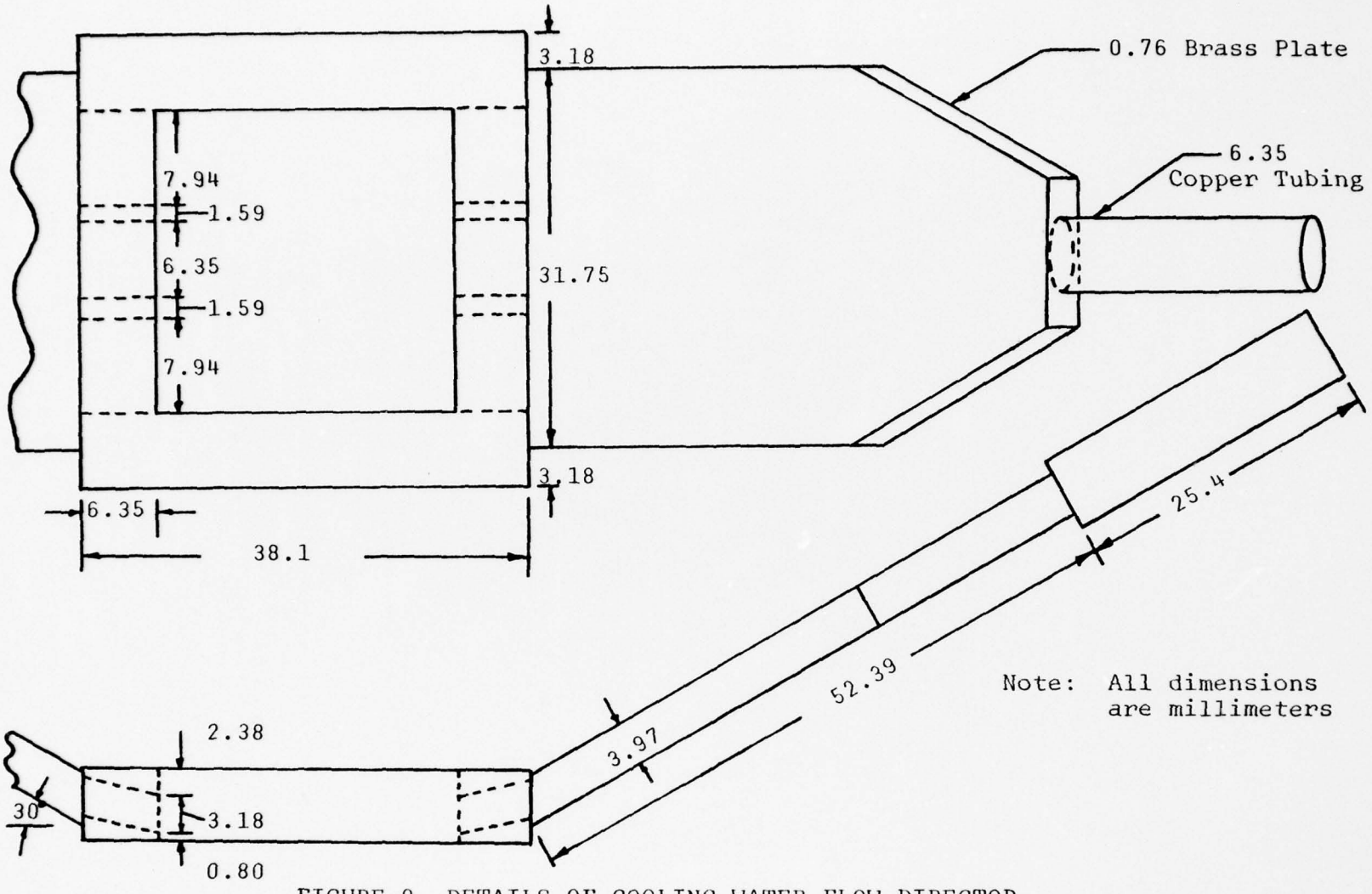

FIGURE 9 DETAILS OF COOLING WATER FLOW DIRECTOR

Note: All dimensions
are millimeters

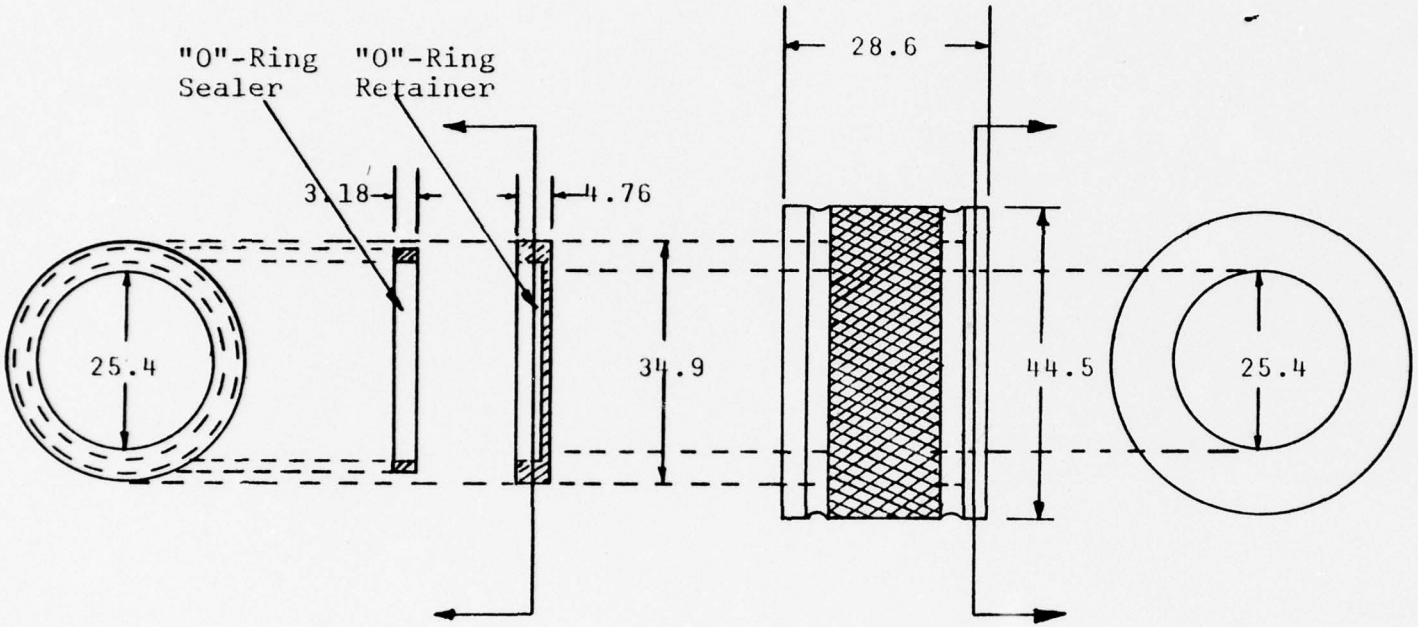

FIGURE 10 DETAILS OF CONDENSER PRESSURE COUPLINGS

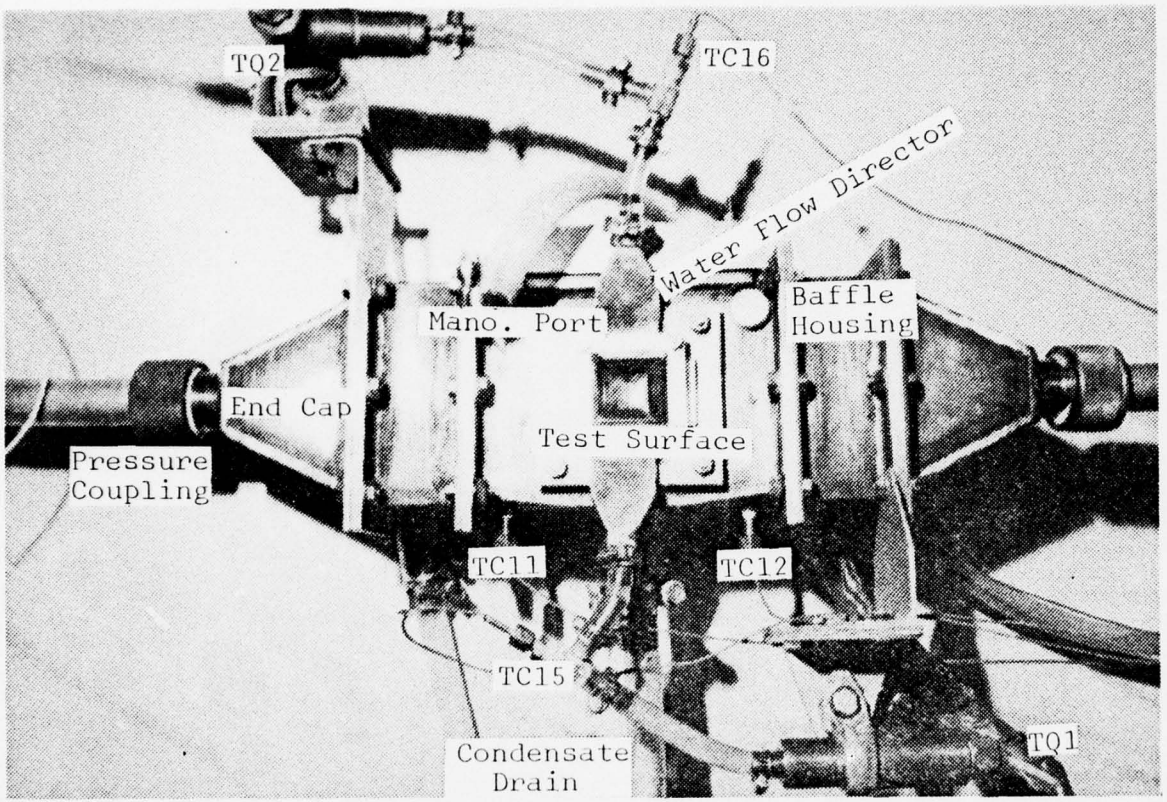

FIGURE 11 CLOSE-UP PHOTOGRAPH OF THE CONDENSER SECTION

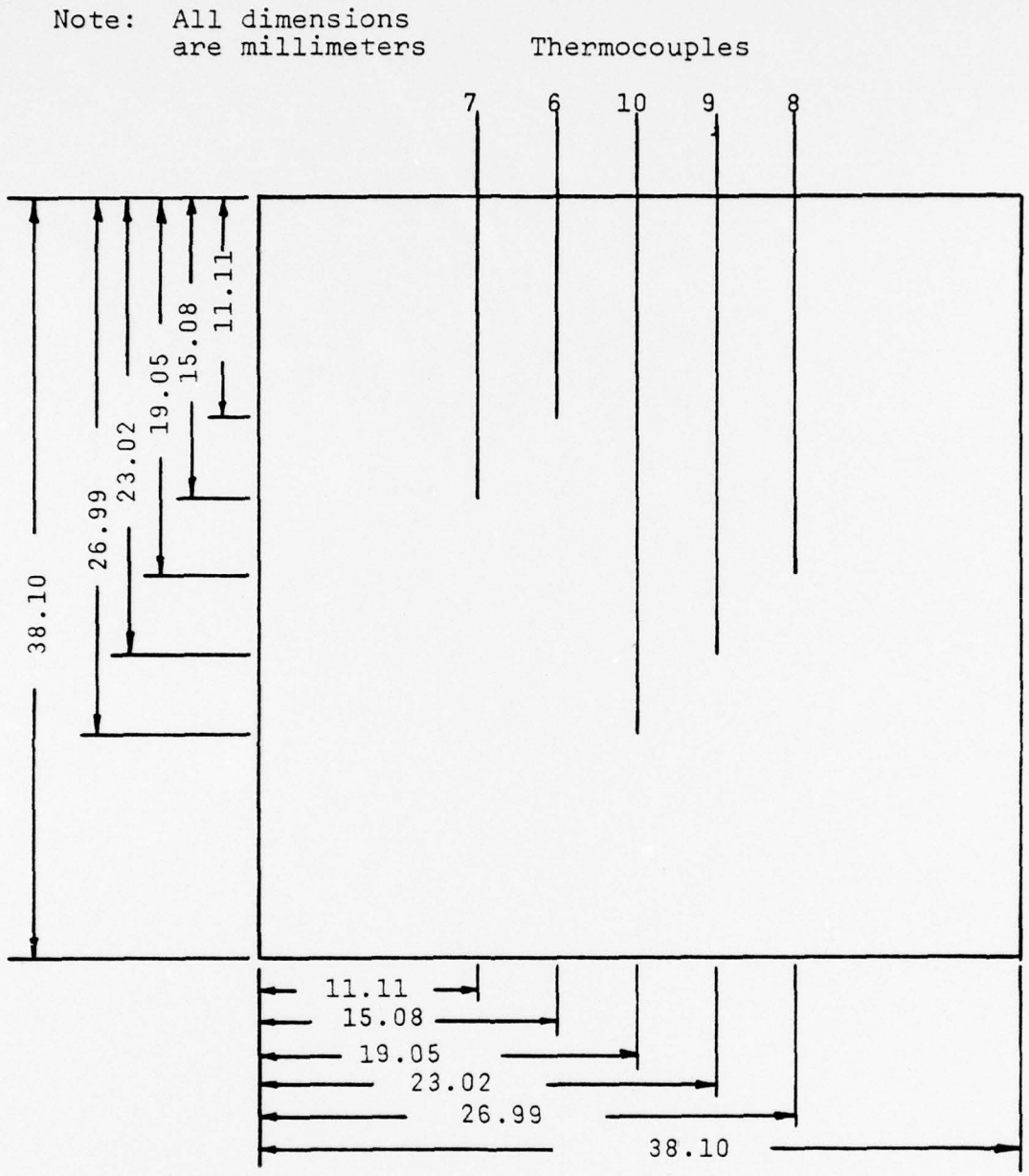

FIGURE 12 THERMOCOUPLE ARRANGEMENT ON TEST SURFACES

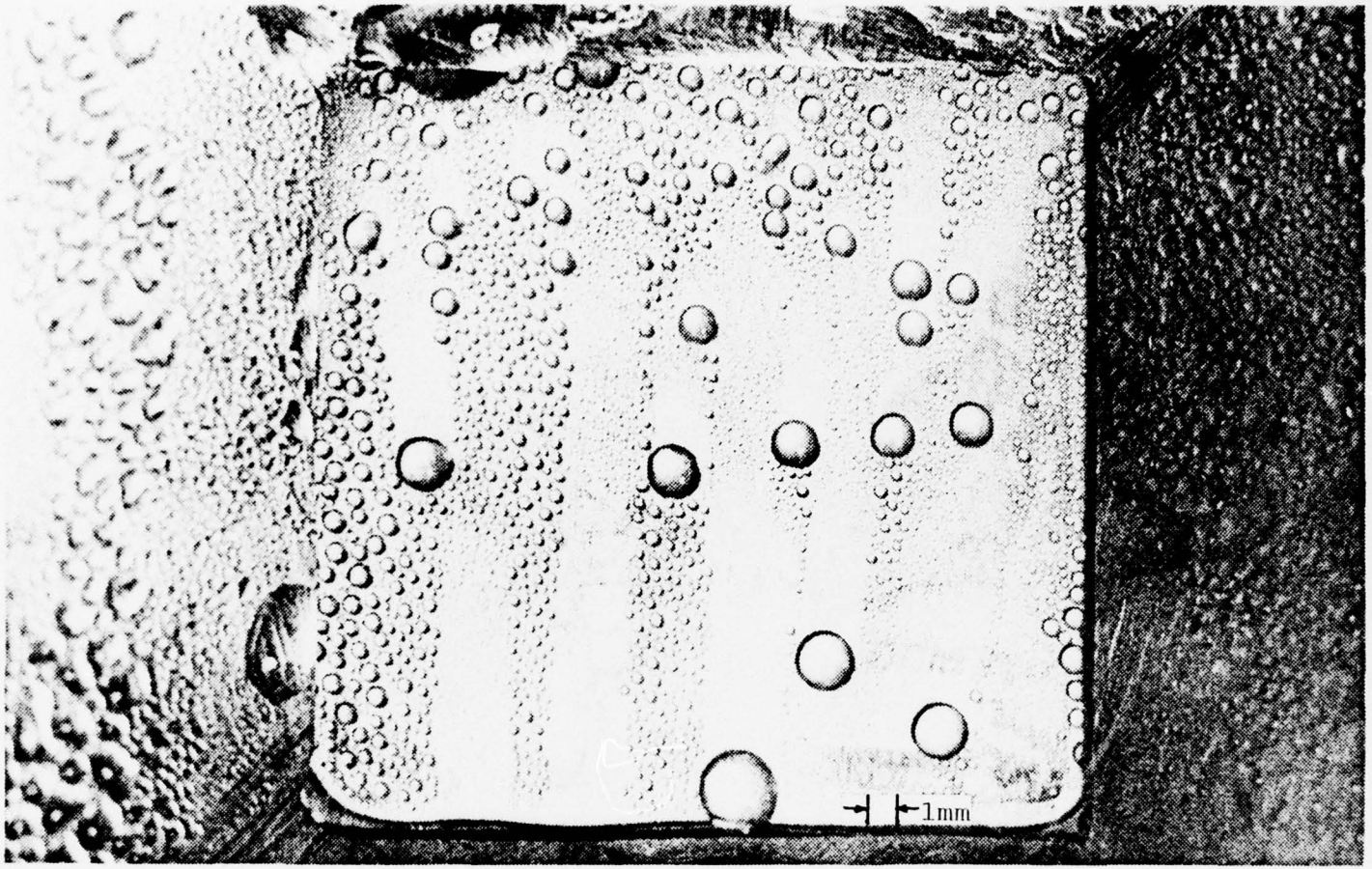

FIGURE 13 PHOTOGRAPH OF DROPWISE CONDENSATION OF STEAM ON A VERTICAL COPPER PLATE WITH A HEAT FLUX OF 460 kW/m^2 AND A ΔT OF 9.1 $^{\circ}$C

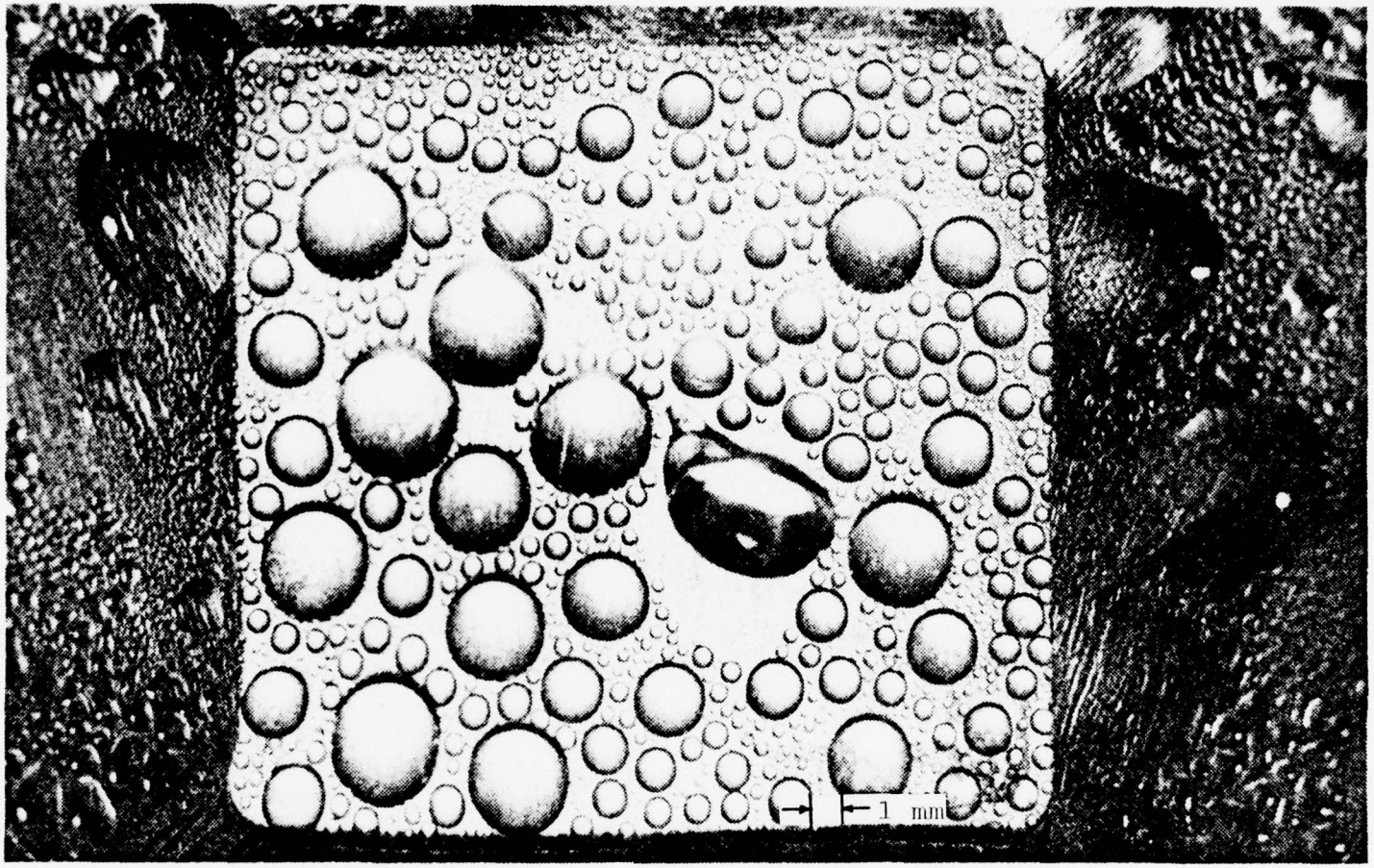

FIGURE 14 PHOTOGRAPH OF DROPWISE CONDENSATION OF STEAM ON A HORIZONTAL (FACING DOWN) COPPER PLATE WITH A HEAT FLUX OF 370 kW/m^2 AND A ΔT OF 19.0 °C

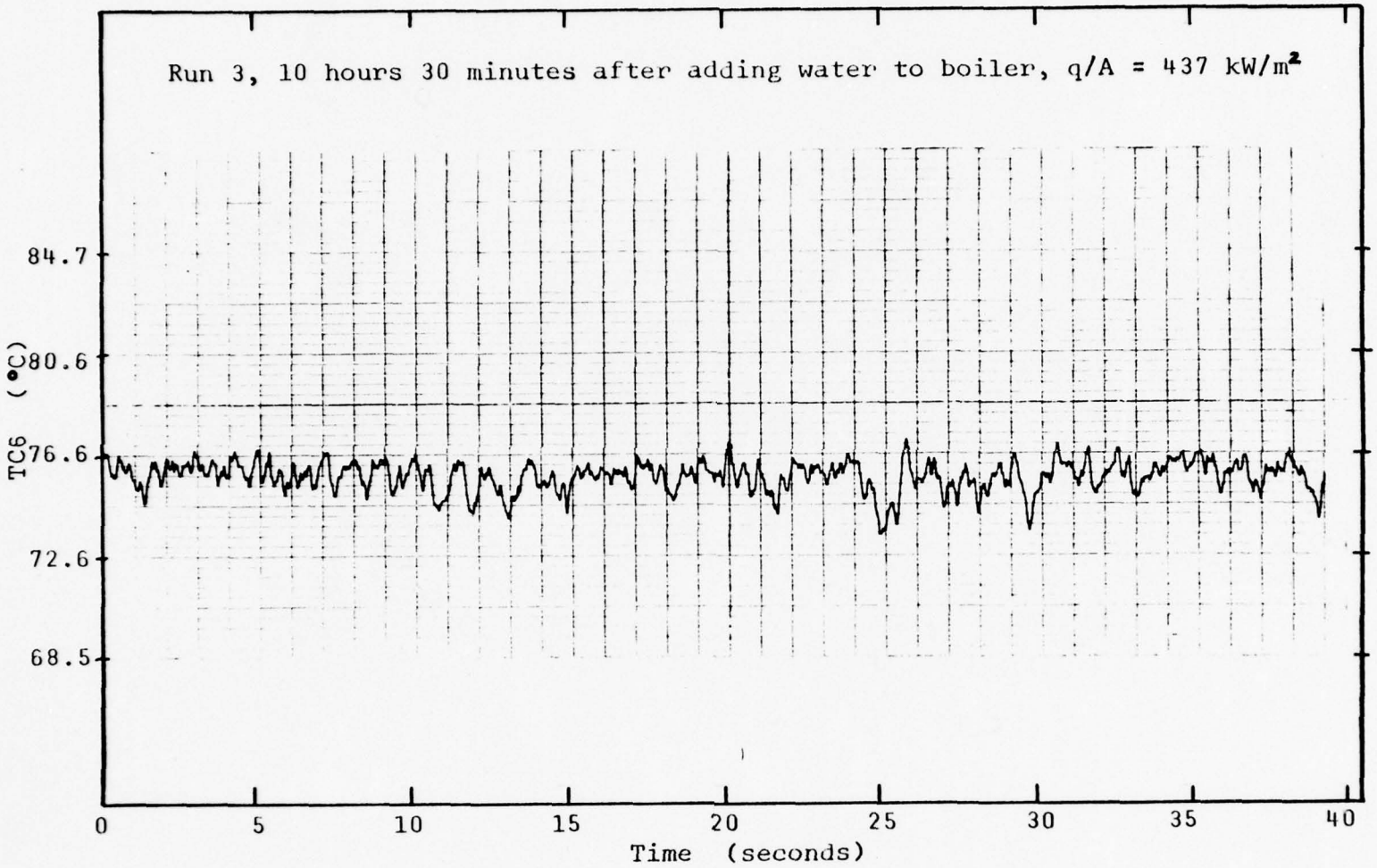

FIGURE 15 TEMPERATURE FLUCTUATION ON 0.051 mm PLAIN COPPER FOIL AS RECORDED BY THERMOCOUPLE 6

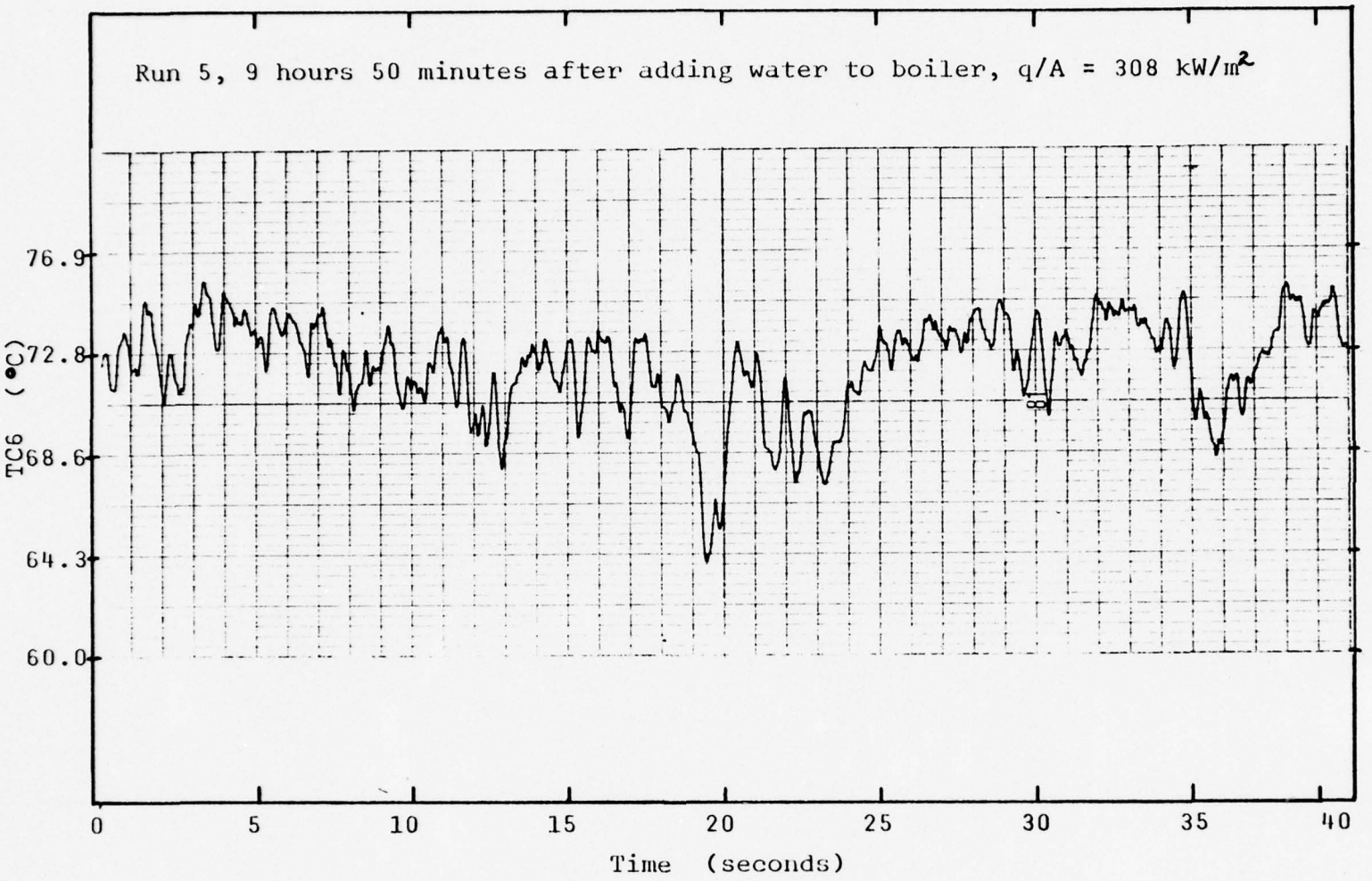

FIGURE 16 TEMPERATURE FLUCTUATION ON 0.051 mm TITANIUM FOIL AS RECORDED BY THERMOCOUPLE 6 AFTER PROLONGED BOILING

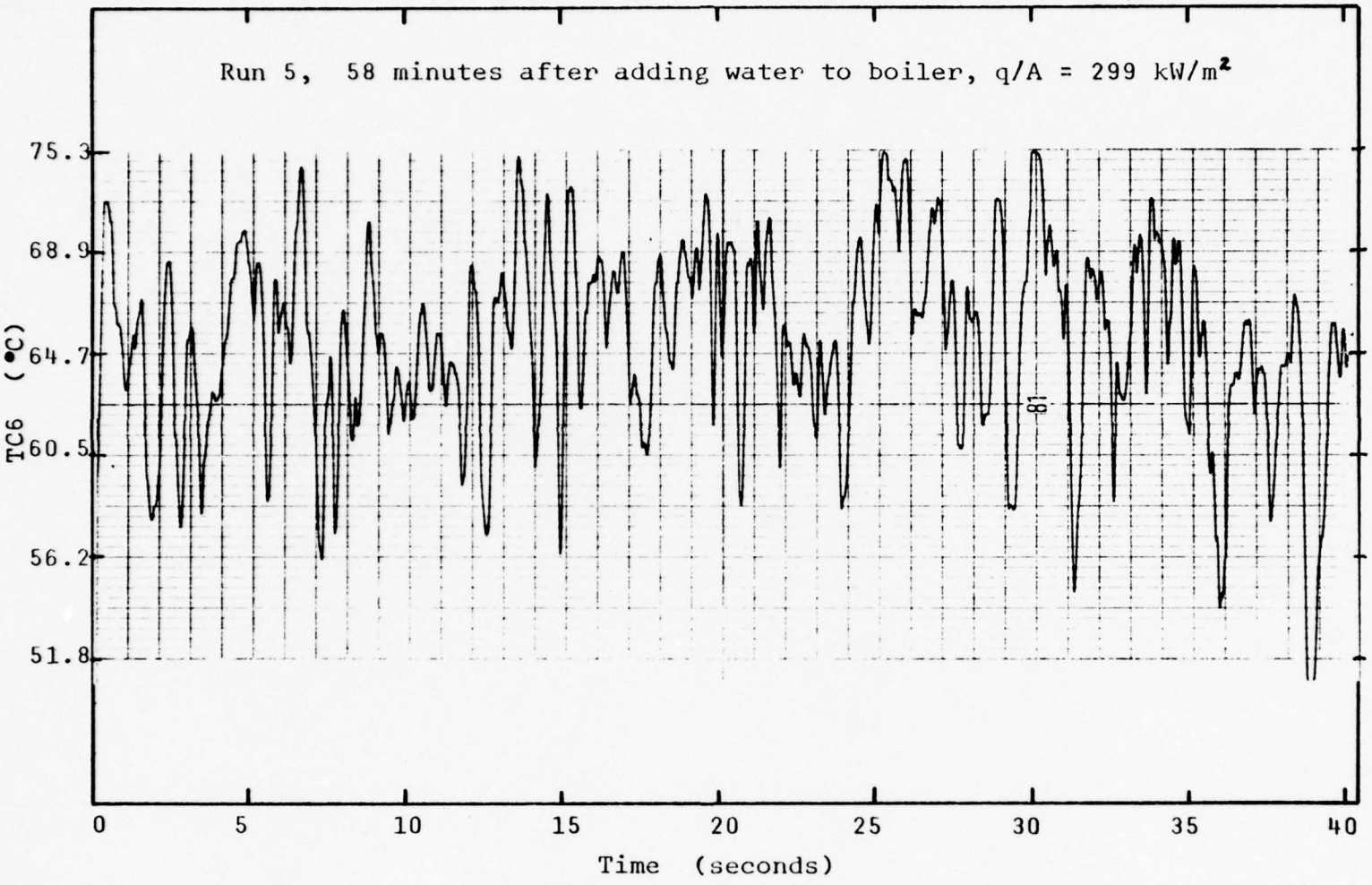

FIGURE 17 TEMPERATURE FLUCTUATION ON 0.051 mm TITANIUM FOIL AS RECORDED BY THERMOCOUPLE 6

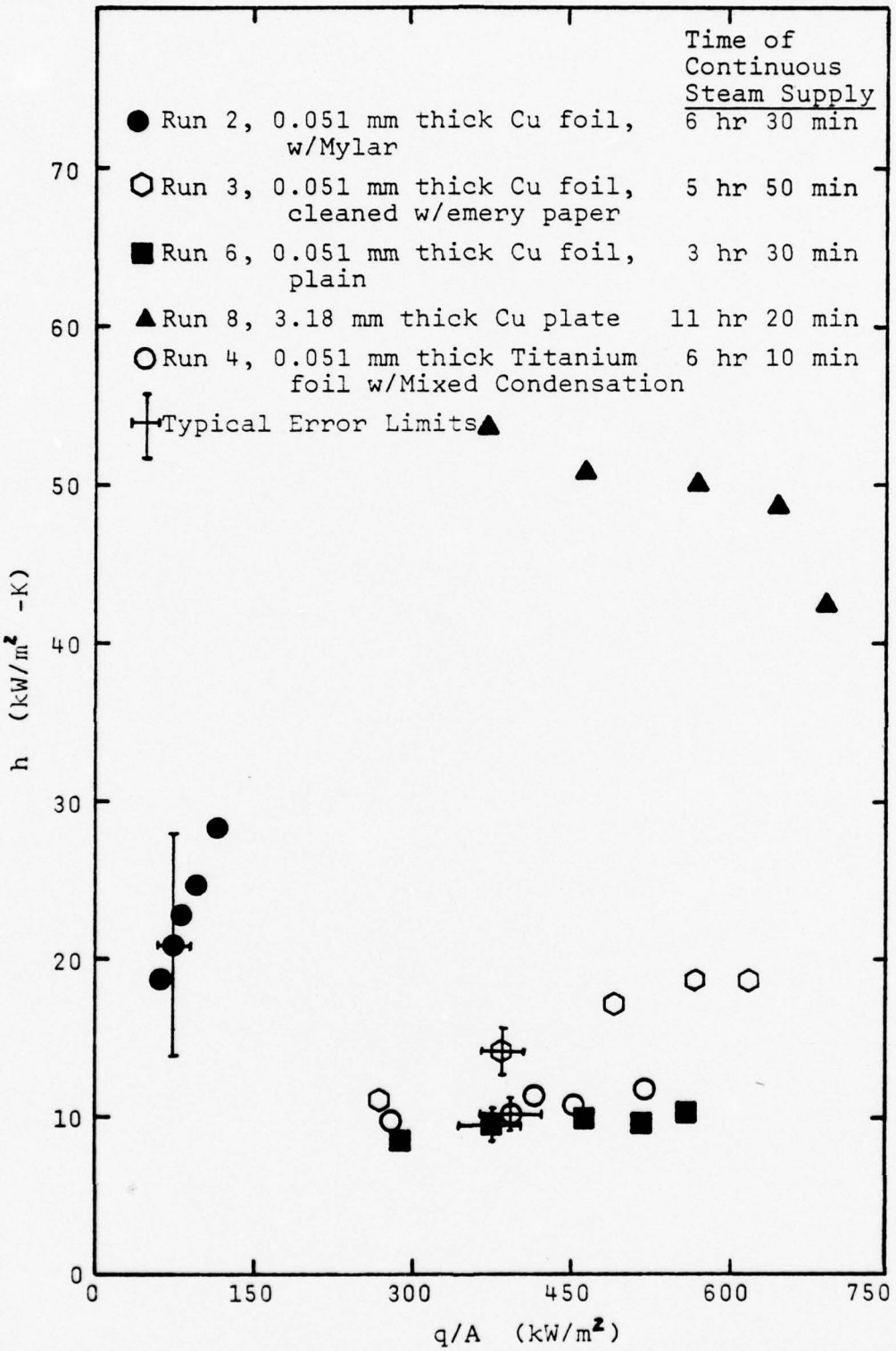

FIGURE 18 EFFECT OF THERMAL RESISTANCE ON HEAT TRANSFER COEFFICIENT DURING DROPWISE CONDENSATION

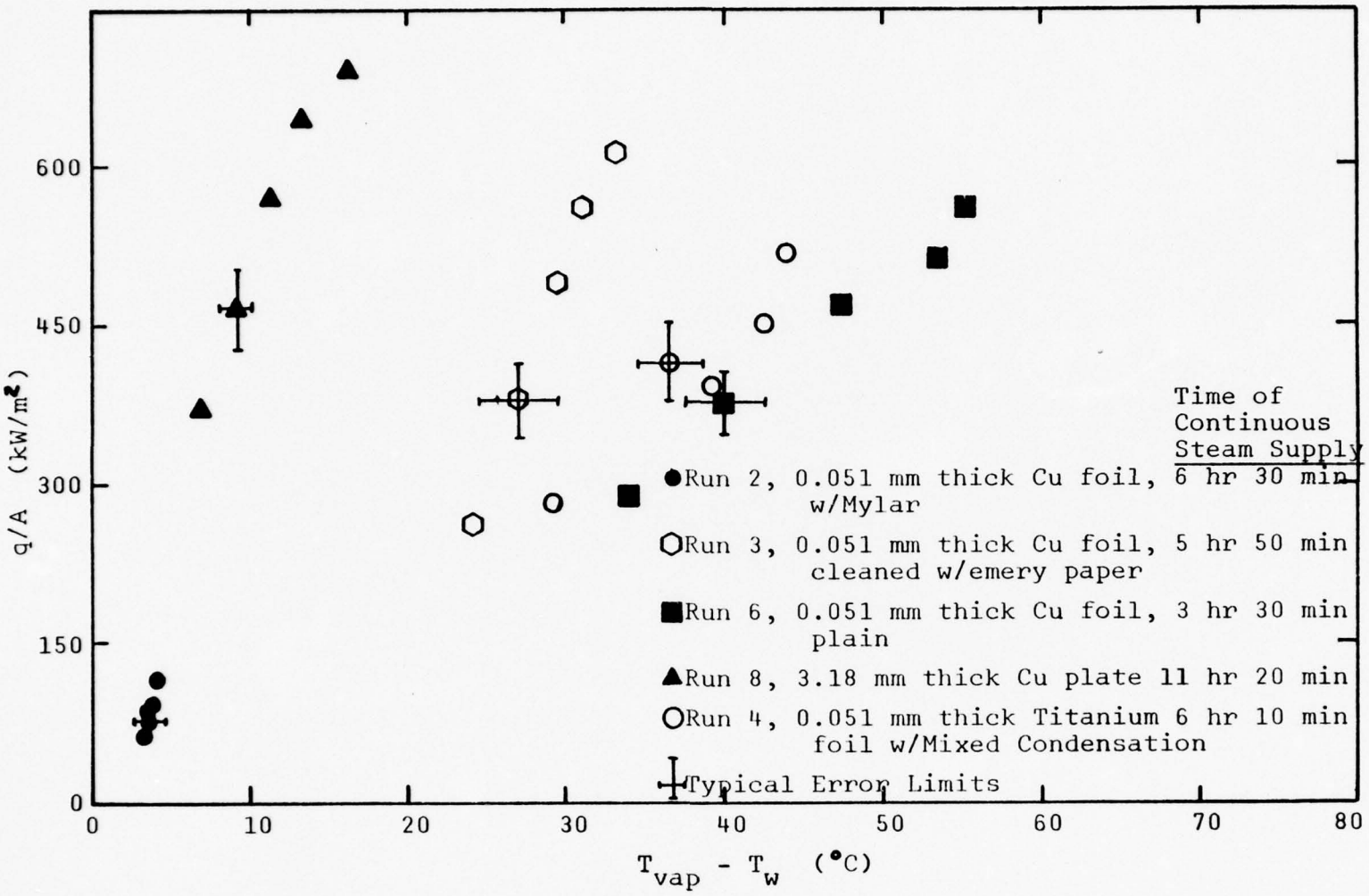

FIGURE 19 HEAT FLUX vs $(T_{vap} - T_w)$ FOR VARYING THERMAL RESISTANCES

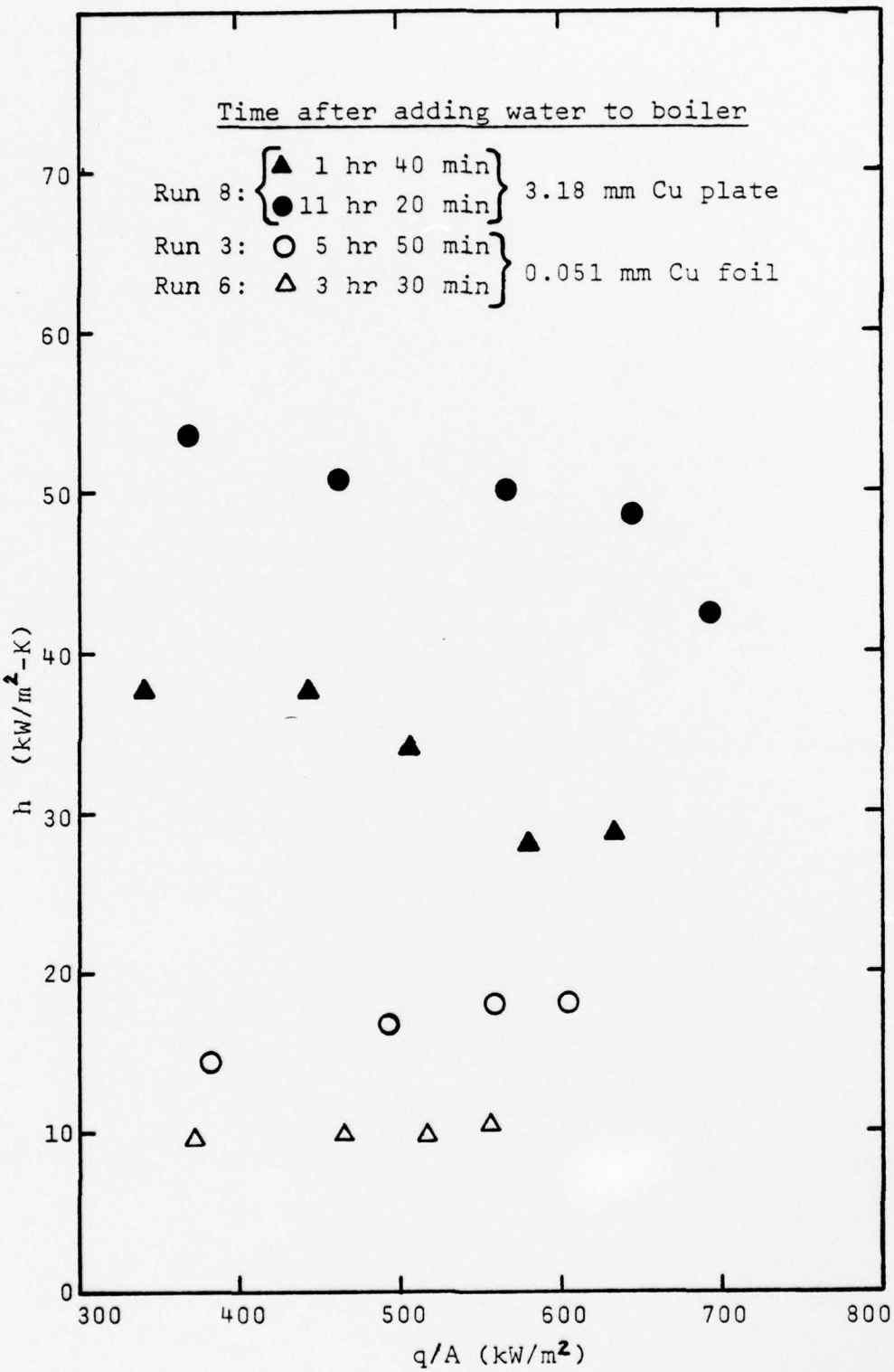

FIGURE 20 EFFECT OF AIR ON HEAT TRANSFER COEFFICIENT DURING DROPWISE CONDENSATION

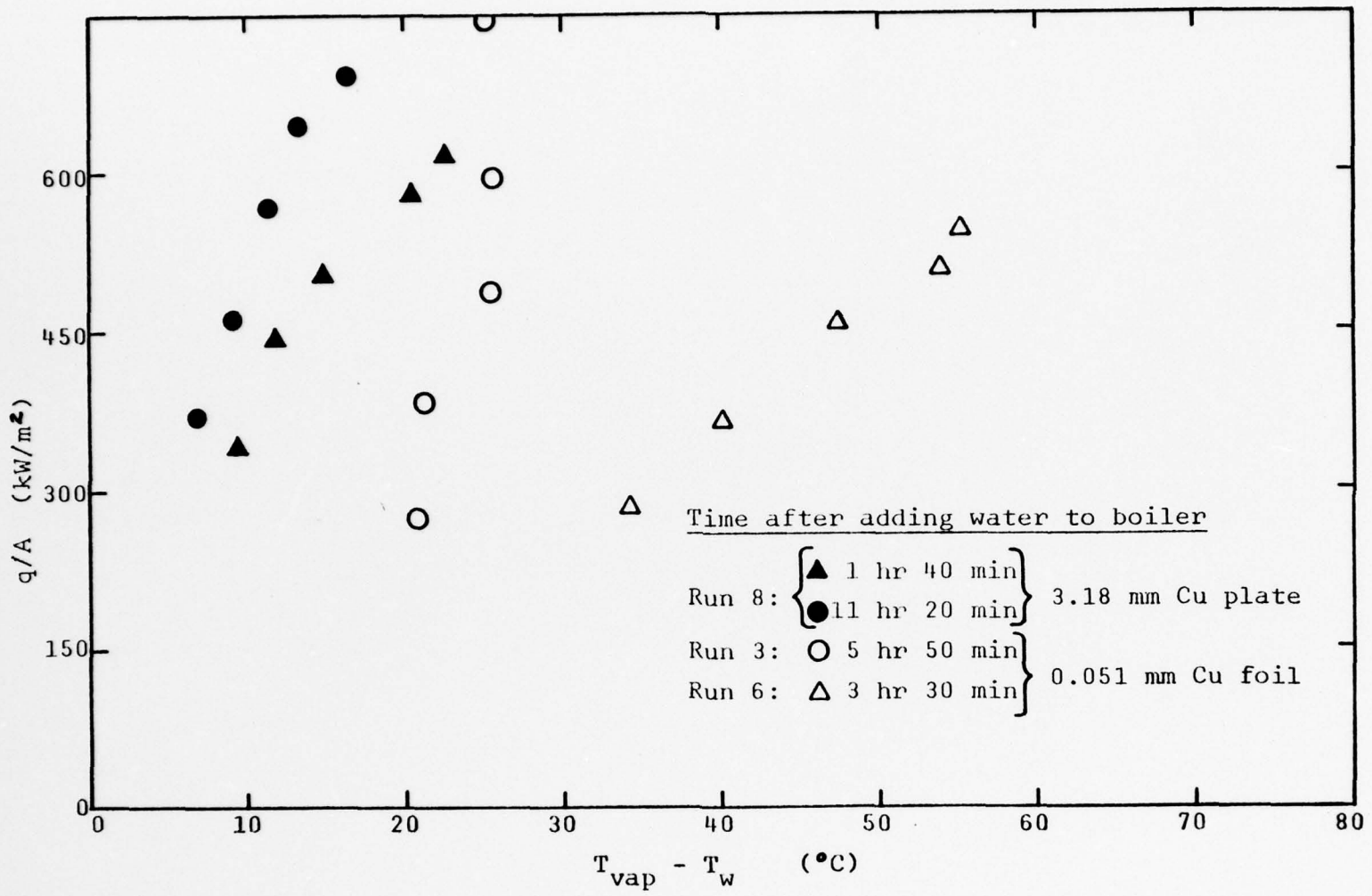

FIGURE 21 EFFECT OF AIR ON HEAT TRANSFER DURING DROPWISE CONDENSATION

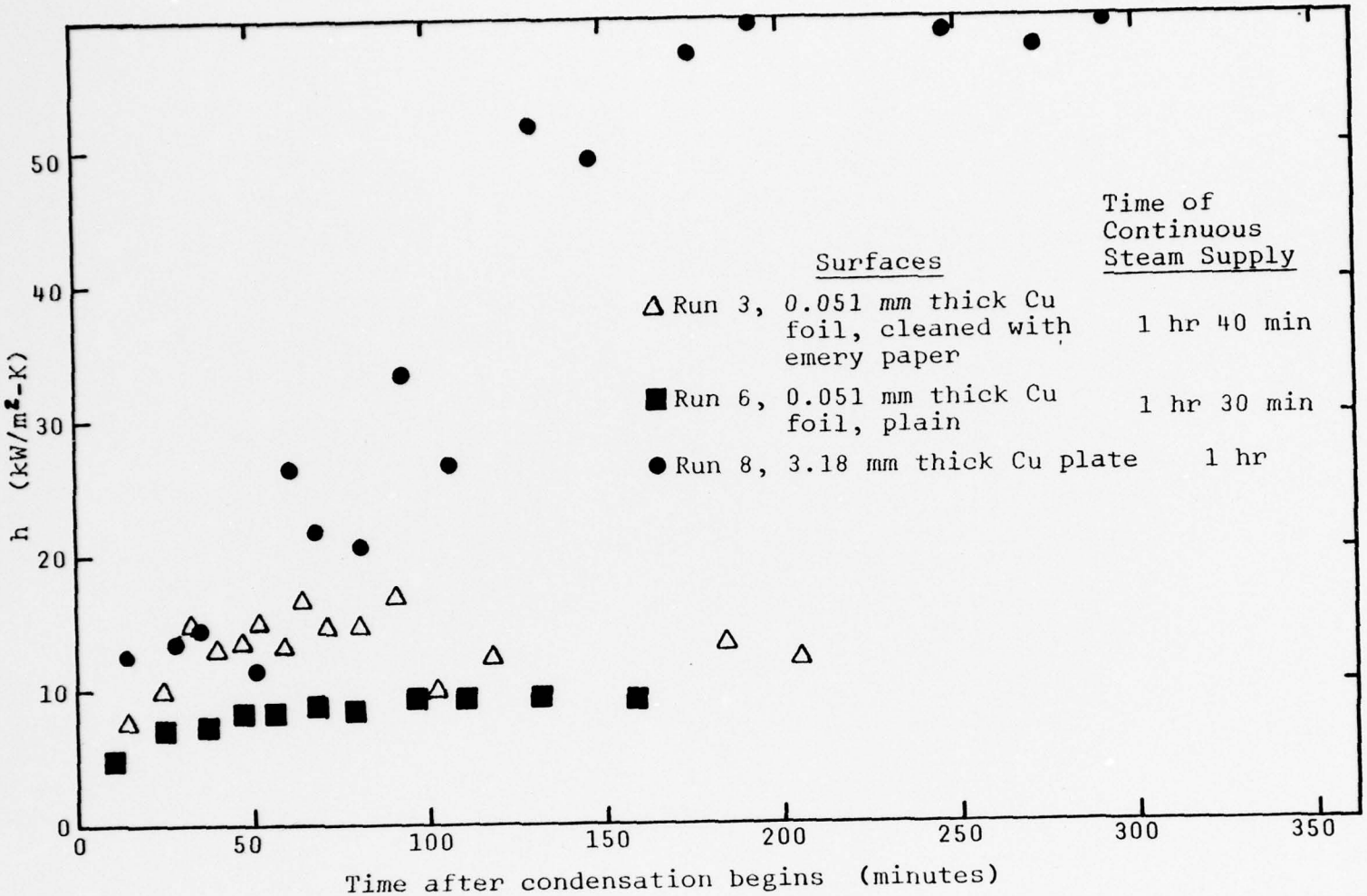

FIGURE 22 VARIATION OF DROPWISE CONDENSATION HEAT TRANSFER COEFFICIENT WITH TIME

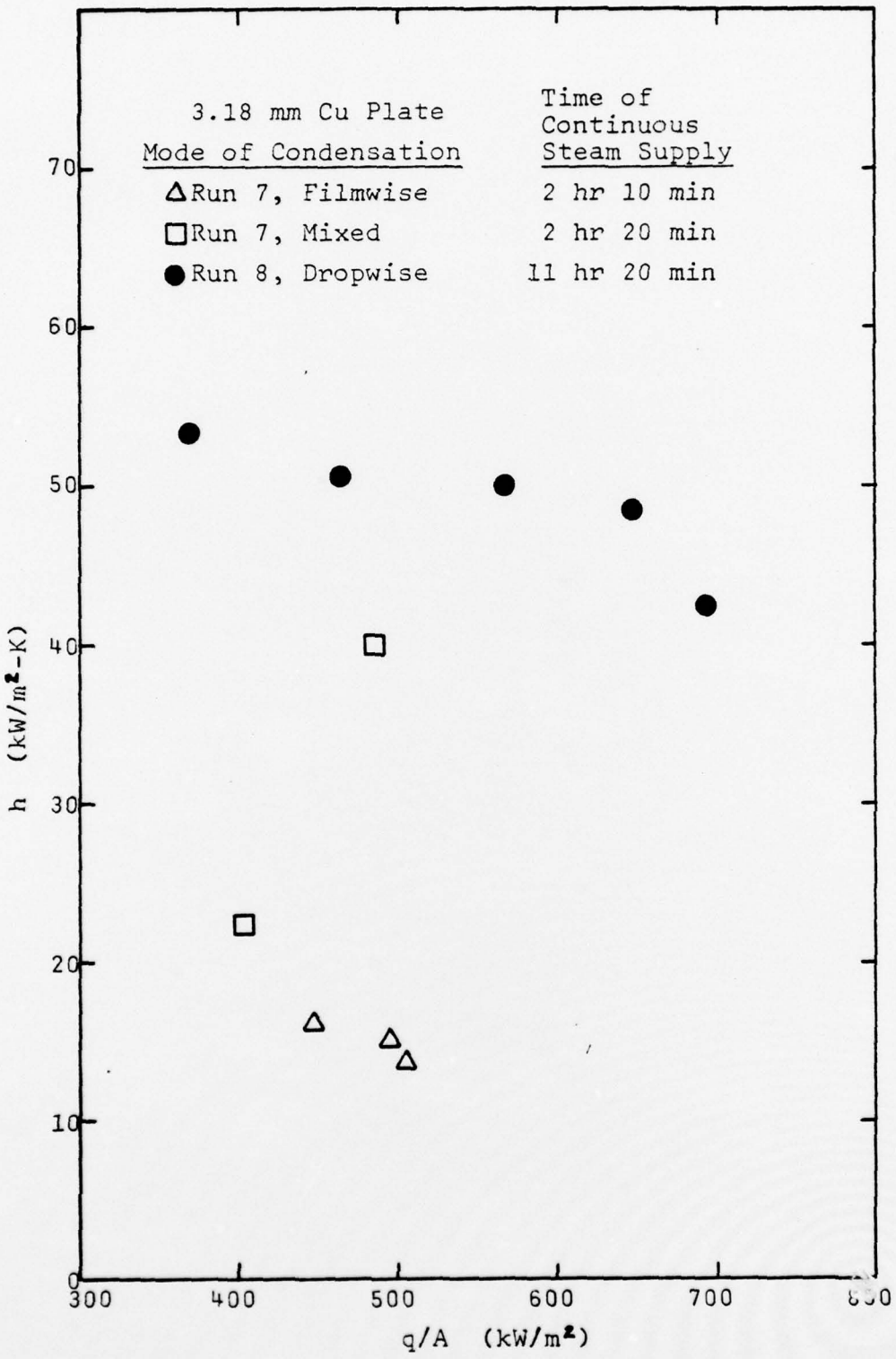

FIGURE 23 HEAT TRANSFER COEFFICIENT vs HEAT FLUX FOR DIFFERENT MODES OF CONDENSATION

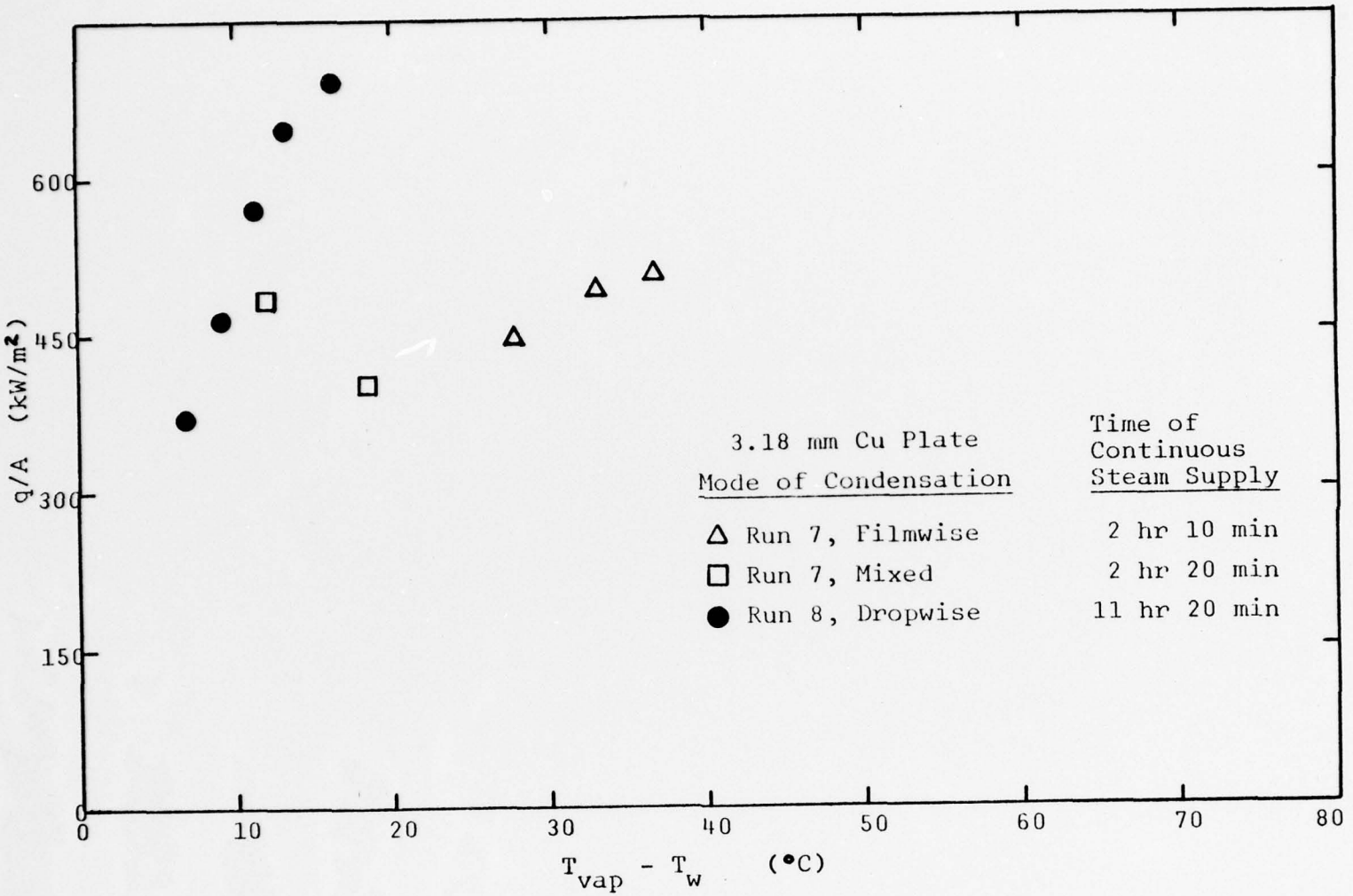

FIGURE 24 HEAT FLUX vs ($T_{vap} - T_w$) FOR DIFFERENT MODES OF CONDENSATION

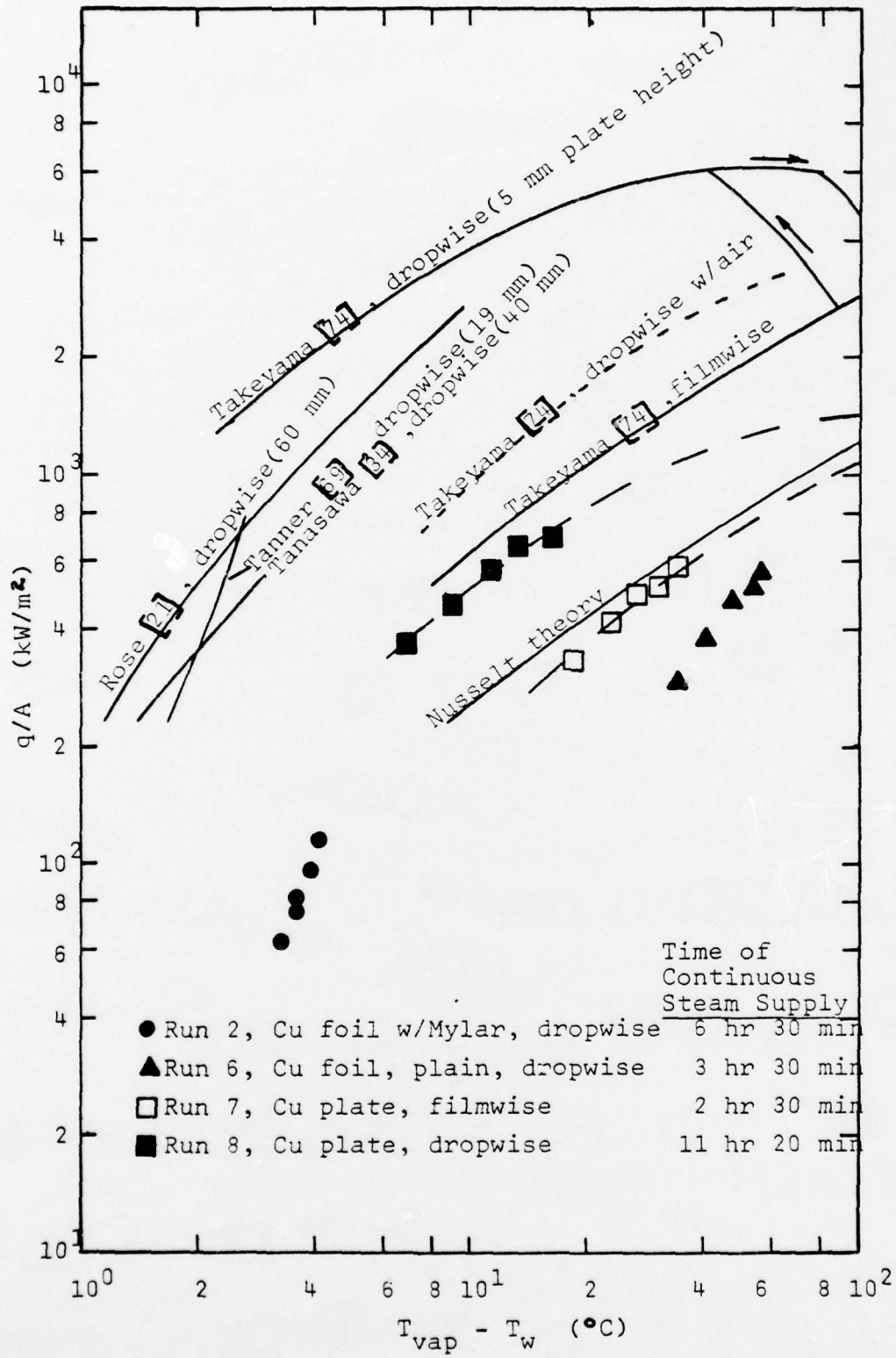

FIGURE 25 COMPARISON OF EXPERIMENTAL DATA WITH THE CONDENSING CURVE AS PROPOSED BY TAKEYAMA [74]

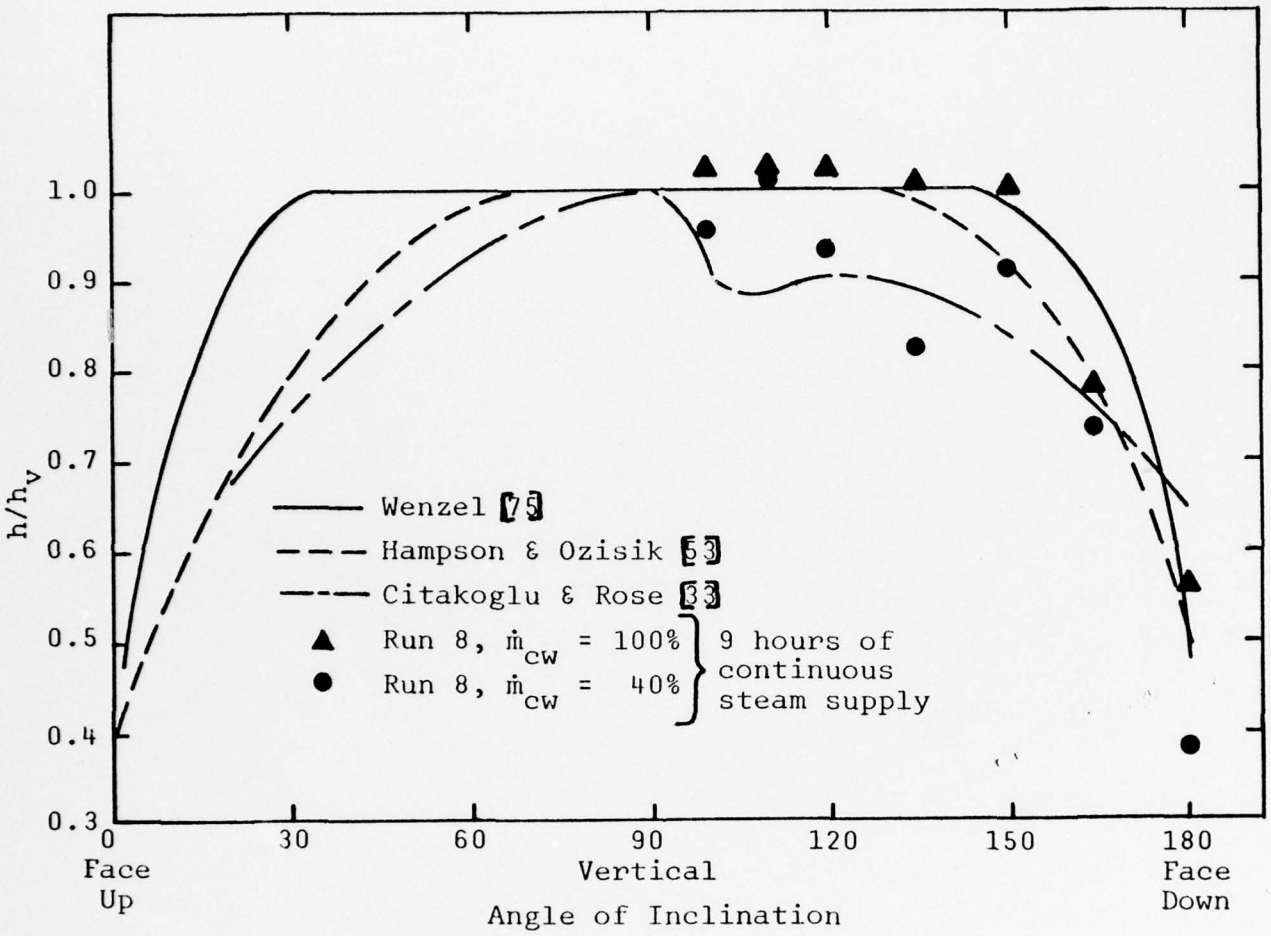

FIGURE 26 VARIATION OF DROPWISE CONDENSATION HEAT TRANSFER COEFFICIENT WITH SURFACE INCLINATION

LIST OF REFERENCES

1. Nusselt, W., "Die Oberflachen kondensation des Wasserdamples," Zeitzchrift des Vereines Deutscher Ingenieure, v. 60, p. 541, 1916.

2. Jakob, M., "Heat Transfer in Evaporation and Condensation — II," Mechanical Engineering, v. 58, p. 729-739, 1936.

3. Holman, J. P., Heat Transfer, 3rd ed., p. 299-304, McGraw-Hill, 1972.

4. Rohsenow, W. M., "Condensation - Part A: Film Condensation," Handbook of Heat Transfer, edited by W. M. Rohsenow and J. P. Hartnett, Chap. 12, Part A, p. 1-33, McGraw-Hill, 1973.

5. Bromley, L. A., Industrial Engineering Chem., v. 44, p. 2966, 1952.

6. Gebhart, B., Heat Transfer, McGraw-Hill, 1961.

7. Schmidt, E., W. Schuring, and W. Sellschoop, "Versuche über die Kondensation von Wasserdampf in Film-und Tropfenform," Tech. Mech. Thermo-Dynam, v. 1, p. 53, 1930.

8. Baer, E., and J. M. McKelvey, "Heat Transfer in Dropwise Condensation," Delaware Science Symposium, University of Delaware, 1958.

9. Welch, J. F., and J. W. Westwater, "Microscopic Study of Dropwise Condensation," International Developments in Heat Transfer, v. 2, p. 302-309, ASME, 1961.

10. Eucken, A., "Energie und Stoffaustausch an Grenzflachen," Naturwissenschaften, v. 25, p. 209, 1937.

11. Kast, W., "Warmeubertragung bei Tropfenkondensation," Chem.-Ingr.-Tech., v. 35, p. 163, 1963.

12. Kast, W., "Bedentung der Keimbildung und der instationaren Warmeubertragung fur den Warmeubertragung bei Blasenverdampfung und Tropfenkondensation," Chem.-Ingr.-Tech., v. 36, p. 933, 1964.

13. Emmons, H., "The Mechanism of Drop Condensation," Transactions American Institute of Chemical Engineers, v. 35, p. 109-125, 1939.

14. Tammann, G., and W. Boehme, "Die Zahl der Wassertropfehen bei der Kondensation auf verschiedenen festen Stoffen," Annalen der Physik, v. 5, p. 77-80, 1935.

15. McCormick, J. L., and E. Baer, "Dropwise Condensation on Horizontal Surfaces," Devel. in Mech. (Proc. of 8th Midwestern Mech. Conf. 1963) 1965.

16. McCormick, J. L., and E. Baer, "On the Mechanism of Heat Transfer in Dropwise Condensation," Journal of Colloid Science, v. 18, p. 208-216, 1963.

17. McCormick, J. L. and J. W. Westwater, "Nucleation Sites for Dropwise Condensation," Chem. Eng. Science, v. 20, p. 1021, 1965.

18. Baer, E., J. A. Koutsky, and A. G. Walton, "The Nucleation of Water Vapor on Surface Films Formed by Absorption on Metal Surfaces," Surface Science, v. 3, p. 280, 1965.

19. Umur, A., and P. Griffith, "Mechanism of Dropwise Condensation," ASME, Paper 64-WA/HT-3, Journal of Heat Transfer, p. 275-282, 1965.

20. Le Fevre, E. J., and J. W. Rose, "A Theory of Heat Transfer by Dropwise Condensation," 3rd International Heat Transfer Conference, Chicago, A.I.Ch.E., v. 2, p. 362-375, 1966.

21. Rose, J. W., "On the Mechanism of Dropwise Condensation," Int. J. Heat Mass Transfer, v. 10, p. 755-762, 1967.

22. Hurst, C. J., Transient Droplet Growth During Dropwise Condensation, Ph.D. Thesis, Penn. State University, 1966.

23. Mikic, B. B., "On Mechanism of Dropwise Condensation," Int. J. Heat Mass Transfer, v. 12, p. 1311-1323, 1969.

24. Graham, C., and W. F. Aerni, "Dropwise Condensation: A Heat Transfer Process for the '70s," Naval Ship System Command Tech. News, v. 19, p. 8-15, July, 1970.

25. Graham, C., The Limiting Heat Transfer Mechanism of Dropwise Condensation, Ph.D. Thesis, Massachusetts Institute of Technology, 1969.

26. Hurst, C. J., and D. R. Olson, "Conduction through Droplets during Dropwise Condensation," ASME, Paper 72-HT-50, 1972.

27. Wilmshurst, R., and J. W. Rose, "Dropwise Condensation — Further Heat-Transfer Measurements," 4th Inter. Heat Trans. Conference, Paper Cs 1.4, 1970.

28. Nijaguna, B. T., and A. H. Abdelmessih, "Precoalescence Drop Growth Model for Dropwise Condensation," ASME, Paper 71-WA/HT-47, 1971.

29. Hannemann, R. J., and B. B. Mikic, "An Analysis of the Effect of Surface Thermal Conductivity on the Rate of Heat Transfer in Dropwise Condensation," Int. J. Heat Mass Transfer, v. 19, p. 1299-1307, 1976.

30. Hannemann, R. J., and B. B. Mikic, "An Experimental Investigation into the Effect of Surface Thermal Conductivity on the Rate of Heat Transfer in Dropwise Condensation," Int. J. Heat Mass Transfer, v. 19, p. 1309-1317, 1976.

31. Aksan, S. N., and J. W. Rose, "Dropwise Condensation — The Effect of Thermal Properties of the Condenser Material," Int. J. Heat Mass Transfer, v. 16, p. 461-467, 1973.

32. Abdelmessih, A. H., A. W. Neumann, and S. W. Yang, "The Effect of Surface Characteristics on Dropwise Condensation," Letters in Heat and Mass Transfer, v. 2, p. 285-292, 1975.

33. Citakoglu, E., and J. W. Rose, "Dropwise Condensation — The Effect of Surface Inclination," Int. J. Heat Mass Transfer, v. 12, p. 645-651, 1969.

34. Tanasawa, I., F. Tachibana, and J. Ochiai, "Dropwise Condensation," Report of the Institute of Industrial Science, University of Tokyo, v. 23, n. 2, August, 1973.

35. LeFevre, E. J., and J. W. Rose, "An Experimental Study of Heat Transfer by Dropwise Condensation," Int. J. Heat Mass Transfer, v. 8, p. -117-1133, 1965.

36. Rose, J. W., "Further Aspects of Dropwise Condensation Theory," to be published in Int. J. Heat Mass Transfer, 1976.

37. NASA Langley Research Center Report NASA TN D-6302, Promotion of Dropwise Condensation of Ethyl Alcohol, Methyl Alcohol, and Acetone by Polytetrafluoroethylene, by C. E. Kirby, July, 1971.

38. Erb, R. A., "Heterogeneous Nucleation in Dropwise Condensation," in Surface Phenomena of Metals, Monograph 28, Society of Chemical Industry, London, p. 383-405, 1968.

39. Erb, R. A., "Dropwise Condensation on Gold - Improving Heat Transfer in Steam Condensers," Gold Bulletin, v. 6, n. 1, p. 2-6, 1973.

40. Erb, R. A., and E. Thelen, "Promoting Permanent Dropwise Condensation," Industrial Engineering Chemistry, v. 57, n. 10, p. 49-52, October, 1965.

41. Davies, G. A., and A. B. Ponter, "The Prediction of the Mechanism of Condensation on Condenser Tubes Coated with Tetrfluoroethylene," Int. J. Heat Mass Transfer, v. 11, p. 375-377, 1968.

42. Ponter, A. B., and I. G. Diah, "Condensation of Vapors of Immiscible Binary Liquids on Horizontal Copper and Polytetrafluoroethylene-Coated Copper Tubes," Warme- und Stoffubertragung, v. 7, n. 2, p. 94-106, 1974.

43. Blackman, L. C. F., M. J. S. Dewar, and H. Hampson, "An Investigation of Compounds Promoting the Dropwise Condensation of Steam," J. Appl. Chem., v. 7, p. 160-171, April, 1957.

44. Blackman, L. C. F., and M. J. S. Dewar, "Promoters for the Dropwise Condensation of Steam," Parts I-IV, J. Chem. Soc., v. 169, p. 162-176, 1957.

45. Osment, B. D. J., D. Tudor, R. M. M. Speirs, and W. Rugman, "Promoters for the Dropwise Condensation of Steam," Trans. Instn. Chem. Engrs., v. 40, p. 152-160, 1962.

46. Watson, R. G. H., J. J. Brunt, and D. C. P. Birt, "Dropwise Condensation of Steam," International Developments in Heat Transfer, Part II, p. 296-301, 1961.

47. Bromley, L. A., J. W. Porter, and S. M. Read, "Promotion of Drop-By-Drop Condensation of Steam from Seawater on a Vertical Copper Tube," AIChE Journal, v. 14, n. 2, p. 245-250, March, 1968.

48. Wilkins, D. G., L. A. Bromley, and S. M. Read, "Dropwise and Filmwise Condensation of Water Vapor on Gold," AIChE Journal, v. 19, n. 1, p. 119-123, January, 1973.

49. Wilkins, D. G., and L. A. Bromley, "Dropwise Condensation Phenomena," AIChE Journal, v. 19, n. 4, p. 839-845, July, 1973.

50. Bromley, L. A., and S. M. Read, "Dropwise Condensation," AIChE Journal, v. 21, n. 2, p. 391-392, March, 1975.

51. Marine Engineering Lab Research and Development Report 71 106, "A Review of Literature on the Promotion of Dropwise Condensation," by. R. M. Fox, 7 July 1964.

52. Garrett, D., "Dropwise Condensation in Evaporators," British Chemical Engineering, v. 3, p. 498-503, September, 1958.

53. Hampson, H., and N. Ozisik, "An Investigation into the Condensation of Steam," Institution of Mech. Engr., Proc (B), v. 1B, n. 7, p. 282-293, 1952.

54. Hampson, H., "Dropwise Condensation on a Metal Surface," Engineering, v. 178, p. 464-469, April 15, 1955.

55. Rivers, A. D., An Experimental Investigation of Nucleate Boiling in Thin Films, M.S.M.E. Thesis, Naval Postgraduate School, Monterey, California, June, 1974.

56. Moreno, J. J., Condensation of Steam at Sub-Atmospheric Pressures on a Vertical, Flat Plate, M.S.M.E. Thesis, Naval Postgraduate School, Monterey, California, 1972.

57. Fergason, J. L., "Liquid Crystals," Scientific American, v. 211, n. 2, p. 77-85, August 1964.

58. Fergason, J. L., "Liquid Crystals in Nondestructive Testing," Applied Optics, v. 7, n. 9, p. 1729-1737, September, 1968.

59. Raad, T., and J. E. Myers, "Nucleation Studies in Pool Boiling on Thin Plates Using Liquid Crystals," AIChE Journal, v. 17, n. 5, p. 1260-1261, September, 1971.

60. Smith, O. W., D. G. Gisser, M. Young, and S. R. Powers, Jr., "Liquid-Crystal Optical Activity for Temperature Sensing," Applied Physics Letters, v. 24, no. 10, p. 453-454, 15 May, 1974.

61. Cooper, T. E., R. J. Field, and J. F. Meyer, "Liquid Crystal Thermography and Its Application to the Study of Convective Heat Transfer," ASME Paper 75-HT-15, Journal of Heat Transfer, v. 97, p. 442-450, August, 1975.

62. Naval Underwater Sound Center Tech. Report 4235, Utilization of Temperature Sensitive Liquid Crystals for Thermal Analysis and an Application to Transducer Investigation, by R. D. Maple, 1972.

63. Astle, B., "Liquid Crystals – A Viable New Medium," Optical Spectra, v. 7, n. 7, p. 35-40, July, 1973.

64. Brown, G. H., and J. W. Doane, "Liquid Crystals and Some of Their Applications," Applied Physics, v. 4, p. 1-15, 1974.

65. Detz, C. M., and R. J. Vermesh, "Nucleation Effects in the Dropwise Condensation of Steam on Electroplated Gold Surfaces," AICHE Journal, v. 22, n. 1, p. 87-93, January, 1976.

66. Liquid Crystal Industries, Inc., Liquid Crystals Instruction Booklet, 1969.

67. Tucker, R. S., Heat Transfer Characteristics of a Rotating Two-Phase Thermosyphon, M.S.M.E. Thesis, Naval Postgraduate School, Monterey, California, p. 21, September, 1974.

68. Griffith, P., and M. S. Lee, "The Effect of Surface Thermal Properties and Finish on Dropwise Condensation," Int. J. Heat Mass Transfer, v. 10, p. 697-707, 1967.

69. Tanner, D. W., D. Pope, C. J. Potter, and D. West, "Heat Transfer in Dropwise Condensation – Part II," Int. J. Heat Mass Transfer, v. 8, p. 427-436, 1965.

70. Tanner, D. W., D. Pope, C. J. Potter, and D. West, "Heat Transfer in Dropwise Condensation at Low Steam Pressure in the Absence and Presence of Non-Condensable Gas," Int. J. Heat Mass Transfer, v. 11, p. 181-190, 1968.

71. Tanner, D. W., C. J. Potter, D. Pope and D. West, "Heat Transfer in Dropwise Condensation – Part I," Int. J. Heat Mass Transfer, v. 8, p. 419-426, 1965.

72. O'Bara, J. T., E. S. Killian, and L. H. S. Roblee, Jr., "Dropwise Condensation of Steam at Atmospheric and Above Atmospheric Pressures," Chemical Engineering Science, v. 22, p. 1305-1314, 1967.

73. Citakoglu, E., and J. W. Rose, "Dropwise Condensation – Some Factors Influencing the Validity of Heat-Transfer Measurements," Int. J. Heat Mass Transfer, v. 11, p. 523-537, 1968.

74. Takeyama, T., and S. Shimizu, "On the Transition of Dropwise-Film Condensation," International Heat Transfer Conference, 5th Proceedings, Tokyo, Japan, Sept. 3-7, 1974, v. 3, Paper Cs 2.5, p. 274-278.

75. Wenzel, H., "Versuch uber Tropfenkondensation," Allg. Warmetech, v. 8, p. 53, 1957.

76. Kline, S. J., and F. A. McClintock, "Describing Uncertainties in Single-Sample Experiments," Mechanical Engineering, v. 75, p. 3-8, January, 1953.

INITIAL DISTRIBUTION LIST

		No. Copies
1.	Defense Documentation Center Cameron Station Alexandria, Virginia 22314	2
2.	Library, Code 0212 Naval Postgraduate School Monterey, California 93940	2
3.	Department of Mechanical Engineering Code 69 Naval Postgraduate School Monterey, California 93940	1
4.	Associate Professor Paul J. Marto Code 69Mx Department of Mechanical Engineering Naval Postgraduate School Monterey, California 93940	1
5.	Kenneth J. Graham, Code 61KG Department of Chemistry and Physics Naval Postgraduate School Monterey, California 93940	1
6.	LT James L. Morgan, USN Supervisor of Shipbuilding, Conversion and Repair, USN San Francisco, California 94135	1